ELSEVIER

Rich dynamics of a predator-prey system with state-dependent impulsive controls switching between two means ☆

Qianqian Zhang [a], Sanyi Tang [a], Xingfu Zou [b,*]

[a] *School of Mathematics and Statistics, Shaanxi Normal University, Xi'an, Shaanxi 710062, PR China*
[b] *Department of Mathematics, University of Western Ontario, London, ON, N6A 5B7, Canada*

Abstract

This paper deals with the control of a prey species (as an unwanted species) in a predator-prey system. We consider a scenario where there are two control means available and they are applied in a state-dependent impulsive way, meaning that when the population of the harmful species is lower than a preset threshold, no control measure will be implemented; while when it reaches the threshold, the two control means will be used either in alternating order or random order. We formulate a general mathematical model for this scenario to evaluate the effect of such a control strategy by exploring the dynamics of this model. We define a one-dimensional map (Poincaré map) and by using the properties of this map, we derive sufficient conditions for the existence and global stability of an order-k periodic solution. By using the analogue of Poincaré criterion and bifurcation theory, we also establish sufficient conditions for a transcritical bifurcation near the predator-free periodic solution. Finally, we apply the results for the general model to two particular cases from two distinct fields: (I) integrated pest control and (II) tumour control with a comprehensive therapy. For (I), theoretical and numerical results show that the outbreak period of the pest is longer when two pesticides are applied randomly than when the alternating strategy is used. For (II), we find that the treatment frequency of drug rotation strategy is lower than that of no drug change strategy, and that the higher the control intensity, the lower the treatment frequency.

1. Introduction

Among the interactions between various biological species in the real worlds, the predator-prey type interactions is an important and yet the most richest and complicated type of interactions. This is because biologically, there are all kinds of predation mechanisms due to the variety of predation natures; and mathematically, dynamical system describing predator-prey interactions are not monotone systems. More than often, the prey species in predator-prey system is a toxic or harmful species that human beings wish control. Two frequently encountered examples of prey-predator interaction between such species are pests and their natural predators, and tumour cells and the effector cells as natural enemies of the tumour cells.

For a prey-predator system where the prey species is an unwanted and/or harmful species, human interventions by various possible control are often implemented to help reduce the harm/damage the prey species may cause. The purpose of such comprehensive controls of harmful species is to keep the number of harmful species within a certain range [31,33,35,39]. In the context of pest control, the most commonly used means in practice is to spray pesticides; while for tumour cells inhibition, taking certain type of tumour inhibiting drug is a common treatment. In either case, the resistance of pests to a pesticide and cancer cells to a drug can easily occur due to the repeated use of the same pesticide or drug. Once such resistance occurs, the control/therapeutic effect will decrease significantly [2,24].

Taking field pest management as an example, long-term use of a single pesticide in the same area will easily result in drug resistance, this is particularly the case for some pyrethroid insecticides and inhalant fungicides. As a consequence of such a drug resistance, the control effect will be greatly reduced after continued long-term use. In order to prevent or slow down the development of pesticide resistance and/or compliment the usage of a pesticide, the following three methods can be considered [36]:

a) rotative applications of different pesticides with different action mechanisms;
b) combining pesticides with the use natural enemies to control pests, as long as such natural enemies are available;
c) implementing control measures more selectively, and correlating the application of pesticide with economic estimates of crop damage and possible negative impact on the natural enemies as the predators.

Recommendation a) is based on a theory that the possibility of a species developing resistance to two or more insecticides is significantly less than that to only one insecticide. This is because different insecticides usually are made of different chemical groups and have different action modes. For b), natural enemies of pests available mainly include frog, ladybug, sandfly, Trichogramma waps, stink bug, yellow edge step, and parasitic fly etc; and attention needs to be paid to the protection of such wanted beneficial species in order to keep their role of inhibiting pests sustainable. The theoretical basis of recommendation c) is lies in the goal of balancing be-

tween the benefit in reducing the damage to corps and the cost both in finance and in ecology (relevant to b)) —a reasonable level of the pest population may be essential for the persistence of its predator(s). The above considerations a)-c) motivate and justify the idea of *rotative and density dependent applications of pesticides.*

Similarly, in the context of tumour treatment, drug resistance will also affect the effectiveness of tumour control. Systemic therapy (including chemotherapy and molecular targeted therapy) is one of the main means to control cancer. However, chemotherapy generally needs to be repeated many times. If the same type of chemical anti-tumour drugs are used every time, some cancer cells may become resistant to the chemotherapeutic drugs [22]. For example, chemotherapy may causes fibroblasts near tumours to produce large amounts of the protein WNT16B, which stimulates the growth of cancer cells which are drug-resistant [3]. Drug resistance may also occur when the same kind of molecular targeted anti-tumour drugs are used for many times.

Just as for the use of pesticides for field pest control discussed above, the rotative use of a variety of chemical anti-tumour drugs or molecular targeted anti-tumour drugs with different mechanisms can slow down drug resistance. The use of other treatment methods can also reduce drug resistance and effectively treat tumours, including surgical resection, radiotherapy, immunotherapy, and a combination of the above methods [14]. State-dependent (or density dependent) impulsive therapy strategy is a common method to treat cancer in experiments and clinics. It means that when the diameter of tumour or the number of tumour cells is lower than a certain threshold, it will not be treated, but once it exceeds the threshold, it will be treated with surgery, chemotherapy, radiotherapy, or immunotherapy [4,9,16,38].

Although pest control and tumour control are two different topics, the above discussions show that the rotative and state-dependent control strategy seem to be a strategy that need to be sought for both of them. If the above state-dependent control strategy is implemented at a time, the populations will change drastically in a short time. Thus, continuous dynamical system models are no longer suitable to describe the population dynamics in such a situation, and *state-dependent impulsive differential systems* offer better and natural choices. Indeed, there have been some prey-predator models with state-dependent feedback control incorporated to characterize and evaluate the strategies in integrated pest control [28,34,37,42,44], in comprehensive treatment of tumours [31,32], in prevention and treatment of infectious diseases [6,23,43], and in treatment of diabetes mellitus [17,40,41].

For example, in [32], the authors propose a feedback control model of immunogenic tumours with comprehensive therapy, in which, once the tumour size reaches a critical value, surgical resection and appropriate immunotherapy are carried out. The results show that this control method can not only control cancer below a certain level, but also maintain the activity of the immune system. In references [34,39], researchers propose a state-dependent impulsive model for integrated pest management. In those models, when the economic threshold (pest control level) was fixed, the killing rate of insecticides to pests and natural enemies remain unchanged, and they obtained the sufficient conditions for the existence and stability of order-1 periodic solutions. In [42], a generalized impulsive Kolmogorov model was used to study the control of harmful species. Through bifurcation analysis, the authors are able to demonstrate how the values of the model parameters corresponding to human intervention measures (including the killing rate of drugs, the constant release number of predators, and the implementation threshold of control measures) affect the dynamic properties of the model.

The aforementioned works have promoted the development of relevant theories of state-dependent impulsive semi-dynamical systems. However, *a common assumption* in those models in the above papers is that the survival rate of harmful species remains the *same constant* after

each impulsive intervention (killing). This can not reflects the characteristic of *rotative use* of different drugs or pesticides that generally have different inhibiting (killing) rates. In this paper, we propose a prey-predator model with impulsive state-dependent controls on the prey (harmful species) by a rotative use of interventions (drugs or pesticides or natural enemies) that allow different inhibiting (killing) rates against the harmful species (prey). To avoid making things too complicated, we work on the scenario of two different interventions, reducing *rotative use* to *alternating use*. Note that "drugs" for control the prey may also be toxic to predators, and hence the impulsive and alternating use of "drugs" will also be reflected on the dynamic equation for the predator. The main purpose of this paper is to study the dynamics of the proposed impulsive prey-predator model with switching state-dependent strategies by using the properties of successor functions (Poincaré maps) and bifurcation theory. Such a study may help us further and better evaluate the effect of drug rotations in the control of harmful species.

The rest of the paper is organized as follows. In Section 2, we formulate the main model and review some useful mathematical lemmas, for readers' convenience. In Section 3, we derive the Poincaré maps for the model and explore its properties. Then we establish some sufficient conditions for existence of order-k periodic solutions and for the global stability of order-1 periodic solutions, and discuss the possibility of the existence of multiple fixed points. In Section 4, we investigate the existence and stability of boundary periodic solution of the proposed model when only a single chemical means is used to control harmful species, and discuss the bifurcations near the boundary periodic solution. In Section 5, to demonstrate the obtained theoretical results, we present some numerical simulation results that are carried out for two particular cases of the model: integrated pest control and tumour treatment. We also use the numerical simulations to show the complexity of model dynamics when two known drugs are *randomly (instead of in alternating order)* selected to control harmful species each time. Finally, we complete the paper with some discussions and remarks on the results of the paper.

2. Model formulation and preliminaries

The basic ODE model employed in our work is the following general predator-prey model of Kolmogorov [1,19,26]:

$$
\begin{cases}
\dfrac{dx(t)}{dt} = x(t)F_1(x(t), y(t)) = P(x(t), y(t)), \\[3mm]
\dfrac{dy(t)}{dt} = y(t)F_2(x(t), y(t)) = Q(x(t), y(t)),
\end{cases}
\tag{2.1}
$$

where $x(t)$ and $y(t)$ represent the populations of the prey and the predator at time t, respectively. Depending on the situation, the prey can be pests or tumour cells, the predator can be natural enemies or effector cells. Here functions $F_1(x, y)$ and $F_2(x, y)$ denote the per capita growth rate of the prey and the predator, respectively. For (2.1), to accommodate the *nature of predator-prey interactions*, we pose the assumptions on $F_1(x, y)$ and $F_2(x, y)$ as in [1]:

(H1) F_1 and F_2 are continuous in $R_+^2 = \{(x, y)|x \geq 0, y \geq 0\}$.
(H2) F_1 and F_2 are continuously differentiable in $R_{+0}^2 = \{(x, y)|x > 0, y > 0\}$.
(H3) There exists positive $\bar{x}$ and $\bar{y}$ such that $(x - \bar{x})F_1(x, 0) < 0$ and $(y - \bar{y})F_1(0, y) < 0$ hold for all $x \geq 0$, $x \neq \bar{x}$, $y \geq 0$, and $y \neq \bar{y}$.

(H4) There exists a positive $\hat{x}$, which satisfies $(x - \hat{x})F_2(x, 0) > 0$ for all $x \geq 0$ and $x \neq \hat{x}$.

(H5) $F_{1y} < 0$ and $F_{2y} \leq 0$ in R^2_{+0}.

(H6) $xF_{1x} + yF_{1y} < 0$ holds for all $(x, y) \in R^2_{+0}$.

(H7) $xF_{2x} + yF_{2y} > 0$ holds for all $(x, y) \in R^2_{+0}$.

The following two assumptions will also be used in Section 3:

(H2)' $F_1, F_2 \in C^2$ in R^2_+.

(H8) $F_{1yy} = 0$ and $F_{2yy} = 0$ for all $(x, y) \in R^2_+$.

Here F_{ix}, F_{iy}, F_{ixx}, or F_{iyy} $(i = 1, 2)$ represent the partial derivatives of respective orders of the function F_i to x or to y.

Since the inequalities in (H3) and (H4) will be repeatedly used in this paper and it involves two constants $\bar{x}$ and $\hat{x}$ which play crucial role in our analysis, they deserve some more detailed explanations. Indeed, (H3) indicate that $\bar{x}$ actually accounts for the *carrying capacity of the prey species* in the absence of the predator; and $\bar{y}$ gives the *maximum population of the predator* that the prey can support; while (H4) means that $\hat{x}$ is the *minimum population of the prey* needed for the predator to survive. The biological interpretations of the other hypotheses mentioned above are shown in literature [26]. Unless otherwise stated, we suppose that assumptions (H1)-(H7) hold in the rest of this paper.

We now incorporate density dependent impulsive control to the system (2.1) by presetting a threshold for the population of the harmful species (prey), denoted by ET. Realistically, such a threshold value should not exceed the carrying capacity of the prey, therefore, in the rest of the paper, we always $ET < \bar{x}$.

When $x(t) < ET$, no control is implemented, while when $x(t) = ET$, an impulsive control is applied to reduce the prey population. For the control, we assume that *there are two choices available*, denoted by (C1) and (C2), which may have different efficacy in reducing the prey population. Let p_1 and p_2 denote the respective efficacy (or killing rate of drug or pesticide) of the two controls. In general, p_1 and p_2 depend on the dosage of the drug or pesticide. The widely used kill efficiency function is an exponential distribution function [5,12,20,25], i.e., $p_1(D) = 1 - e^{-\lambda_1 D}$ and $p_2(D) = 1 - e^{-\lambda_2 D}$, where D is the dosage of the drug or pesticide, λ_1 and λ_2 are constants. Considering that a control aiming to reduce the prey population may also have some negative impact on the predator that may cause some deaths of the predators, we introduce two more parameters q_1 and q_2 to denote such negative side effect. In the mean time, in addition to applying one of the controls aiming to reduce the prey at the threshold ET, we also accommodate the possibility of releasing certain number of predators, denoted by $\tau \geq 0$. The above scenario leads to the following model:

$$\begin{cases} \dfrac{dx(t)}{dt} = x(t)F_1(x(t), y(t)), \\[2mm] \dfrac{dy(t)}{dt} = y(t)F_2(x(t), y(t)), \end{cases} \quad \text{if } x(t) < ET, \tag{2.2}$$

subject to the control of either

$$(\text{C1}): \begin{cases} x(t^+) = (1 - p_1)x(t), \\[2mm] y(t^+) = (1 - q_1)y(t) + \tau, \end{cases} \quad \text{if } x(t) = ET \tag{2.3}$$

or

$$(C2): \begin{cases} x(t^+) = (1 - p_2)\, x(t), \\ y(t^+) = (1 - q_2)y(t) + \tau, \end{cases} \quad \text{if } x(t) = ET. \tag{2.4}$$

Note that by their meanings, we should have $p_i \in (0, 1)$ and $q_i \in [0, 1)$, $i = 1, 2$. Without loss of generality, we assume $p_1 > p_2$. Here $x(t^+)$ and $y(t^+)$ denote the numbers of the prey and the predator after an integrated control strategy is applied at time t, respectively. We also assume that the initial values (x_0, y_0) of (2.2) satisfies $y_0 = y(0^+) \geq 0$ and $x_0 = x(0^+) < ET$; otherwise, the initial integrated control can be implemented to achieve these. For biological reason, we only focus on the region $V = \{(x, y): \ 0 \leq x < \bar{x}, 0 \leq y\}$.

There comes the issue of how to arrange (C1) and (C2) every time when $x(t)$ reaches the threshold state. In this paper, we propose three strategies:

(S1): *alternating* order starting with the *weaker* one $\{C2, C1, C2, C1, C2, C1, \ldots\}$;
($\overline{\text{S1}}$): *alternating* order starting with the *stronger* one $\{C1, C2, C1, C2, C1, C2, \ldots\}$;
(S2): (C1) and (C2) are applied randomly when $x(t) = ET$ with the probability of applying (C1) being $\bar{P}$ and the probability of applying (C2) being $1 - \bar{P}$.

In the case of two insecticides for (C1) and (C2), they may come from different chemical groups with different modes of action, and it is such a difference together with the rotated uses that may help prevent the occurrence of drug resistance. Since strategies (S1) and ($\overline{\text{S1}}$) are essentially the same, we only analyze (2.2)-(2.3)-(2.4) under the strategy (S1) in this paper. Strategy (S2) means that the two insecticides are applied randomly each time, with a constant probability $\bar{P}$ for (C1) to reflect the user's possible preference based on the information about the two insecticides. Theoretically analyzing the consequences of strategy (S2) requires a new setting that involves probability arguments, as such, we will only briefly explore it numerically to gain some comparison with the alternating order of uses, hoping to motivate some future research projects.

Since (2.1) is the baseline equation of our state-dependent impulsive control model (2.2)-(2.4), its properties are crucial and helpful for us to explore the dynamics of our model (2.2)-(2.4). Below we gather those properties of (2.1) needed for our later analysis, from the literature (see, e.g., [1,19,26]). Lemma 2.1 [1] gives the position of vertical and horizontal isoclinics and the equations to be satisfied, as shown in Fig. 2.1. Lemma 2.2 [1] gives the stability of the equilibrium of model (2.1).

Lemma 2.1. *If functions $F_1(x, y)$ and $F_2(x, y)$ satisfy conditions (H1)-(H7), then*

(i) *$F_1(x, y) = 0$ defines a unique continuous function $y = \varphi_1(x)$ on $[0, \bar{x}]$ such that $\varphi_1(0) = \bar{y}$ and $\varphi_1(\bar{x}) = 0$. Further, function φ_1 is both positive definite and differentiable on $(0, \bar{x})$ and satisfies $\varphi_1'(x) < \varphi_1(x)/x$;*

(ii) *$F_{2x} > 0$ holds for any $(x, y) \in R_{+0}^2$ and $F_2(x, y) = 0$ defines a unique continuous function $x = \varphi_2(y)$ on $[0, +\infty)$ such that $\varphi_2(0) = \hat{x}$. Moreover, φ_2 is differentiable on $(0, +\infty)$ and satisfies $0 \leq \varphi_2'(y) < \varphi_2(y)/y$.*

Lemma 2.2. *Under hypotheses (H1)-(H7), model (2.1) always has equilibria $(0, 0)$ and $(\bar{x}, 0)$ with $(0, 0)$ being unstable. Moreover,*
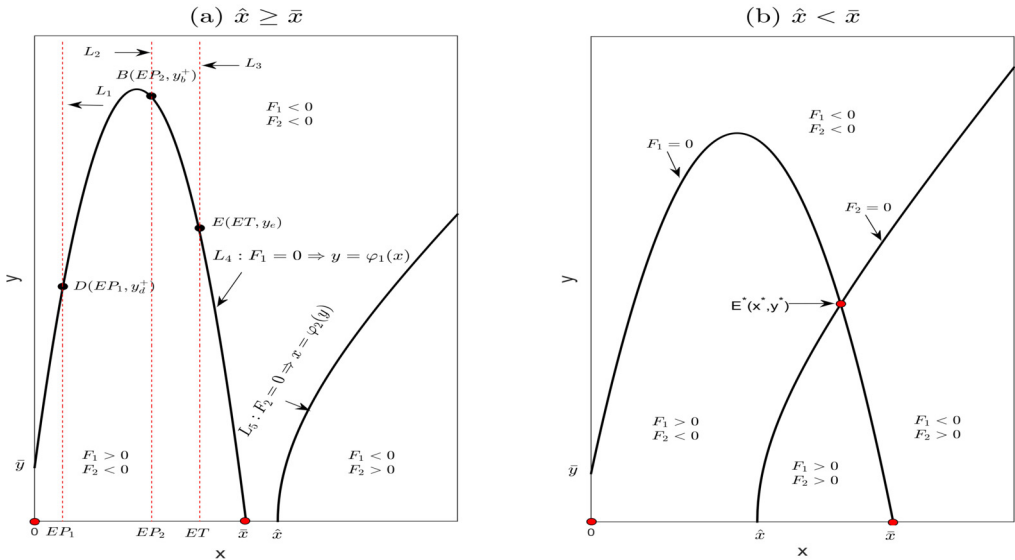
Fig. 2.1. Schematic diagram of functions $F_1(x, y)$ and $F_2(x, y)$ satisfying (H1)-(H7) in (2.1).

(i) when $\hat{x} \geq \bar{x}$ holds, then $(\bar{x}, 0)$ is globally stable in R_{+0}^2;

(ii) when $\hat{x} < \bar{x}$, $(\bar{x}, 0)$ becomes unstable and there exists a unique positive equilibrium $E^* = (x^*, y^*)$ with $\hat{x} \leq x^* < \bar{x}$ which is globally attractive in R_{+0}^2 provided that there is no periodic orbit in R_{+0}^2; and if E^* is unstable then there is at least one limit cycle in R_{+0}^2.

The following lemma [30] is helpful for judging the stability of periodic solutions.

Lemma 2.3 (Analogue of Poincaré's criterion). *For the following impulsive system*

$$
\begin{cases}
\left.\begin{array}{l}
\dfrac{dx(t)}{dt} = P(x(t), y(t)), \\[2mm]
\dfrac{dy(t)}{dt} = Q(x(t), y(t)),
\end{array}\right\} & \text{if } \phi(x(t), y(t)) \neq 0, \\[6mm]
\left.\begin{array}{l}
x(t^+) = x(t) + a(x(t), y(t)), \\[2mm]
y(t^+) = y(t) + b(x(t), y(t)),
\end{array}\right\} & \text{if } \phi(x(t), y(t)) = 0,
\end{cases}
\tag{2.5}
$$

where P, Q, ϕ, a, and b are continuous functions from R^2 into R and $\nabla\phi(x, y) \neq 0$. If $(\xi(t), \eta(t))$ is a periodic solution with period T, then it is orbitally asymptotically stable if the Floquet multiplier μ_2 satisfies $|\mu_2| < 1$, where

$$
\mu_2 = \prod_{n=1}^{q} \triangle_n \exp\left[\int_0^T P_x(\xi(t), \eta(t))dt\right] \exp\left[\int_0^T Q_y(\xi(t), \eta(t))dt\right]
\tag{2.6}
$$

with

$$\Delta_n = \frac{P_+ \left(\frac{\partial b_n}{\partial y} \frac{\partial \phi}{\partial x} - \frac{\partial b_n}{\partial x} \frac{\partial \phi}{\partial y} + \frac{\partial \phi}{\partial x} \right) + Q_+ \left(\frac{\partial a_n}{\partial x} \frac{\partial \phi}{\partial y} - \frac{\partial a_n}{\partial y} \frac{\partial \phi}{\partial x} + \frac{\partial \phi}{\partial y} \right)}{P \frac{\partial \phi}{\partial x} + Q \frac{\partial \phi}{\partial y}}. \tag{2.7}$$

Here, q is the total number of pulses of the periodic solution within the period T, $\tau_n (n \in \mathbb{N})$ is the time of the n-th jump, $a_n = x(\tau_n^+) - x(\tau_n)$, $b_n = y(\tau_n^+) - y(\tau_n)$, $P_+ = P(\xi(\tau_n^+), \eta(\tau_n^+))$, $Q_+ = Q(\xi(\tau_n^+), \eta(\tau_n^+))$, and the rest of Δ_n are calculated at the pulse point $(\xi(\tau_n), \eta(\tau_n))$.

To address the bifurcation of the Poincaré map defined in the next section, we introduce the following lemma [13].

Lemma 2.4 (*Transcritical bifurcation*). *Let $\Phi : U \times I \longrightarrow R$ define a one-parameter family of maps, where $\Phi(y, \alpha)$ is C^r with $r \geq 2$, and U, I are open intervals of the real line containing 0. Assume that*

$$\Phi(0, \alpha) = 0 \text{ for all } \alpha, \quad \Phi_y(0, \alpha^*) = 1, \quad \Phi_{y\alpha}(0, \alpha^*) \neq 0, \quad \Phi_{yy}(0, \alpha^*) > 0 \ (resp. \ < 0).$$

Then there are $\alpha_1 < \alpha^* < \alpha_2$ and $\varepsilon > 0$ such that

(*i*) *if $\alpha_1 < \alpha < \alpha^*$ and $\Phi_{y\alpha}(0, \alpha^*) > 0$ (or $\alpha^* < \alpha < \alpha_2$ and $\Phi_{y\alpha}(0, \alpha^*) < 0$), then Φ has two fixed points, 0 and $y_1(\alpha) > 0$ (resp. $y_1(\alpha) < 0$) in $(-\varepsilon, \varepsilon)$. The origin is asymptotically stable, the other fixed point is unstable;*

(*ii*) *if $\alpha^* < \alpha < \alpha_2$ and $\Phi_{y\alpha}(0, \alpha^*) > 0$ (or $\alpha_1 < \alpha < \alpha^*$ and $\Phi_{y\alpha}(0, \alpha^*) < 0$), then Φ has two fixed points, 0 and $y_1(\alpha) < 0$ (resp. $y_1(\alpha) > 0$) in $(-\varepsilon, \varepsilon)$. The origin is unstable, the other fixed point is asymptotically stable.*

According to the relationship between ET (action threshold), $\bar{x}$ (the carrying capacity of prey), and $\hat{x}$ (the minimum number of prey to ensure predator reproduction), we study the existence and stability of the periodic solutions of hybrid system (2.2)-(2.4) for the following two cases in the rest of this paper:

$$(A) \quad ET < \min\{\bar{x}, \hat{x}\}; \quad (B) \quad \hat{x} < ET < \bar{x}. \tag{2.8}$$

3. Poincaré maps and its properties

In this section, assume $ET < \min\{\bar{x}, \hat{x}\}$ and strategy (S1) is applied in the state-dependent impulsive model (2.2)-(2.4).

The following three vertical lines and two curves are needed in defining Poincaré map and studying its properties:

$$\begin{cases} L_1 : x = (1 - p_1)ET \doteq EP_1, \quad L_2 : x = (1 - p_2)ET \doteq EP_2, \quad L_3 : x = ET, \\ L_4 : F_1(x, y) = 0 \Longrightarrow y = \varphi_1(x), \quad L_5 : F_2(x, y) = 0 \Longrightarrow x = \varphi_2(y), \end{cases}$$

where L_1 and L_2 represent the two phase lines, L_3 represents the impulse line, L_4 is the vertical isocline of model (2.2), and L_5 denotes the horizontal isocline, (see Lemma 2.1). As shown in Fig. 2.1 and Fig. 3.1, the intersection points of vertical isocline L_4 and straight lines L_1, L_2, and L_3 are marked as $D(EP_1, y_d^+)$, $B(EP_2, y_b^+)$, and $E(ET, y_e)$, respectively.
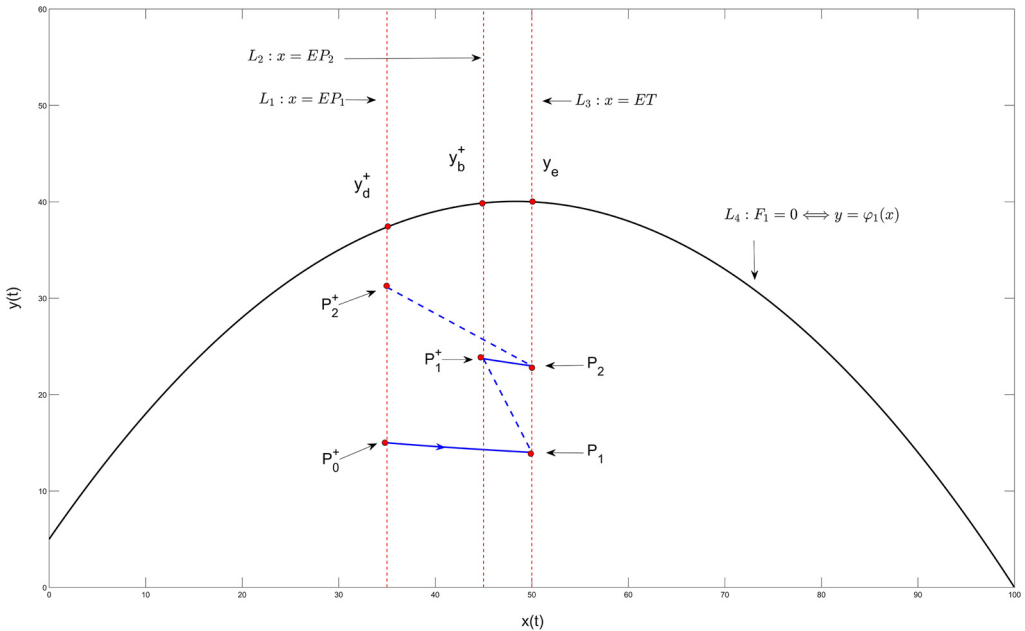
Fig. 3.1. Phase diagram of (2.2)-(2.4) when $ET < \min\{\bar{x}, \hat{x}\}$ and strategy (S1) is applied.

3.1. The definition of Poincaré maps

Let L_1 be the Poincaré section of the system (2.2)-(2.4). For any given point on L_1, denoted by $P_0^+ = (EP_1, y_0^+)$, the trajectory of (2.2) starting from P_0^+ will intersect the threshold line L_3 at a point denoted by $P_1 = (ET, y_1)$. The value y_1 depends on y_0^+ and is denoted as $y_1 = G_1(y_0^+)$. Then, the control (C2) will pull this point to a point on the line L_2, denoted by $P_1^+ = (EP_2, y_1^+)$ where

$$y_1^+ = (1 - q_2)y_1 + \tau = (1 - q_2)G_1(y_0^+) + \tau. \tag{3.1}$$

Trajectory of (2.2) starting from P_1^+ will also intersect the L_3 at a point denoted by $P_2 = (ET, y_2)$ where y_2 depends on y_1^+, denoted as $y_2 = G_2(y_1^+)$. Then, the second control (C1) in (S1) will pull P_2 to the line L_1 at a point $P_2^+ = (EP_1, y_2^+)$ with

$$y_2^+ = (1 - q_1)y_2 + \tau = (1 - q_1)G_2(y_1^+) + \tau. \tag{3.2}$$

Now, combining (3.1) and (3.2), we obtain a map $\Phi : [0, \infty) \to [0, \infty)$ given by

$$\Phi(y) = (1 - q_1)G_2[(1 - q_2)G_1(y) + \tau] + \tau, \quad y \geq 0. \tag{3.3}$$

We call Φ the Poincaré map of (2.2)-(2.4) under strategy (S1).

In the sequel, we follow the convention to denote Φ^n as the n-th iteration of Φ, that is,

$$\Phi^0(u) = u, \quad \Phi^n(u) = \Phi^{n-1}(\Phi(u)), \text{ for } n = 1, 2, ... \tag{3.4}$$

As is customary, a point $u \in [0, \infty)$ is said to be a k-periodic point (periodic point with period k) of Φ, if $\Phi^j(u) \neq u$ for all $1 \leq j < k$ and $\Phi^k(u) = u$. In particular, a 1-periodic point of Φ is nothing but a fixed point of Φ.

Definition 3.1. Assume (S1) is applied. For a $P_0^+(EP_1, y_0^+)$ on the L_1, the corresponding orbit consisting of trajectories $\overparen{P_0^+ P_1}$ and $\overparen{P_1^+ P_2}$ and the two line segments $\overline{P_1 P_1^+}$ and $\overline{P_2 P_2^+}$, as shown in Fig. 3.1, is said to be an order-1 periodic solution of system (2.2)-(2.4) if $P_2^+ = P_0^+$, i.e., y_0^+ is a fixed point of Φ. Similarly, if Φ has a k-periodic point in $[0, \infty)$, then we say the system (2.2)-(2.4) has an order-k periodic solution.

3.2. The properties of the Poincaré map

Let

$$y_d^+ = \varphi_1(EP_1), \quad y_b^+ = \varphi_1(EP_2), \quad \text{and} \quad y_e = \varphi_1(ET).$$

Define

$$y_{d+1} = G_1(y_d^+), \quad y_{d+1}^+ = (1 - q_2)y_{d+1} + \tau, \quad y_b = (y_b^+ - \tau)/(1 - q_2), \qquad (3.5)$$

where G_1 is defined in (3.1). Note that when $\tau < y_b^+ < y_{d+1}^+$, there is a point (ET, y_b) on L_3 and the backward orbit Γ_1 initiating from (ET, y_b) will reach two points (EP_1, y_f^+) and (EP_1, y_g^+) of phase curve L_1 with $y_f^+ < y_d^+ < y_g^+$.

The following theorem presents some properties of Φ.

Theorem 3.1. Assume $ET < \min\{\bar{x}, \hat{x}\}$ and (S1) is applied in (2.2)-(2.4). Then the properties of map $\Phi(u)$ are as follows.

(i) Φ is continuously differentiable on interval $[0, +\infty)$.

(ii) When $y_{d+1}^+ \leq y_b^+$, Φ is increasing on $[0, y_d^+)$ and decreasing on $[y_d^+, +\infty)$. The map Φ is concave down on $(0, y_d^+)$ if (H2)' and (H8) hold.

(iii) When $y_b^+ \leq \tau$, Φ is decreasing on $[0, y_d^+)$ and increasing on $[y_d^+, \infty)$.

(iv) When $\tau < y_b^+ < y_{d+1}^+$, Φ is increasing on $[0, y_f^+) \cup [y_d^+, y_g^+)$ and decreasing on $[y_f^+, y_d^+) \cup [y_g^+, +\infty)$ with $\Phi(y_f^+) = \Phi(y_g^+)$. The map Φ is concave down on $(0, y_f^+)$ if (H2)' and (H8) hold.

(v) $y = \Phi(0)$ is the horizontal asymptote of $\Phi(u)$ as $u \to +\infty$, as shown in Fig. 3.2.

Proof. *Continuous differentiability.* It follows from Lemma 2.2 that if $ET < \min\{\bar{x}, \hat{x}\}$ holds, then any trajectory of model (2.1) starting from the phase curve L_1 or L_2 will reach the pulse curve L_3 in a finite time. Thus, the domain of Φ is $[0, +\infty)$. Φ is continuously differentiable because of the theorem of the continuity and the differentiability of the solution of the ordinary differential equation to the initial value.
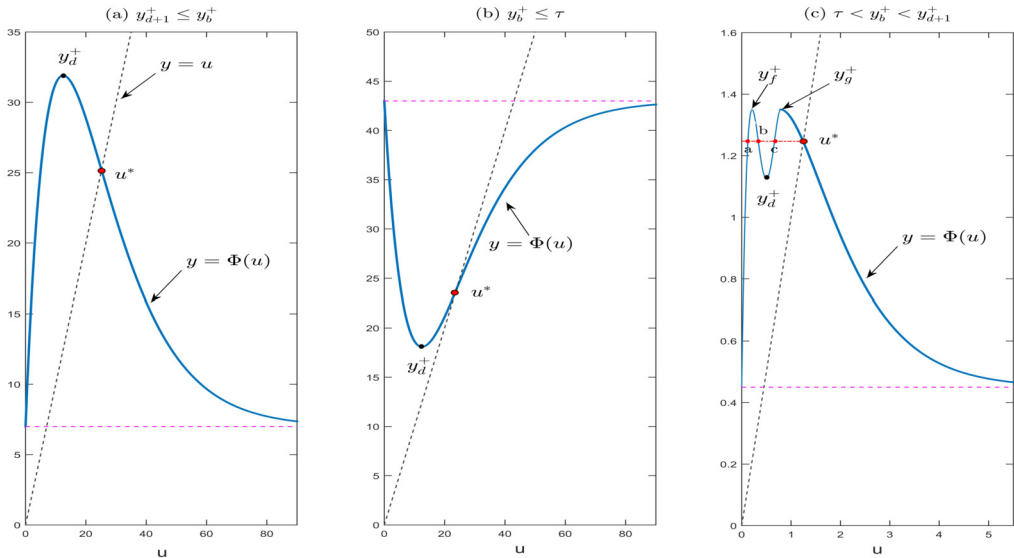
Fig. 3.2. The shape of the Poincaré map Φ when $ET < \min\{\bar{x}, \hat{x}\}$ and (S1) is applied.

Next we prove the respective *monotonicity and concavity* of $\Phi(u)$ on the respective intervals specified in (ii)-(iv). Note from (3.3), i.e., $\Phi(u) = (1 - q_1)G_2(h(u)) + \tau$, where

$$h(u) := (1 - q_2)G_1(u) + \tau, \qquad (3.6)$$

that the range of function h and the monotonicity of continuous functions h and G_2 jointly affect the monotonicity of Poincaré map Φ.

According to the definition of function $G_1(u)$ and the direction of the trajectory when $ET < \min\{\bar{x}, \hat{x}\}$ holds, we get that $G_1(u)$ and $h(u)$ are increasing on $(0, y_d^+)$ and decreasing on $(y_d^+, +\infty)$, and thus the range of $h(u)$ is $[h(0), h(y_d^+)] = [\tau, y_{d+1}^+]$. Similarly, function $G_2(u)$ is increasing on $(0, y_b^+)$ and decreasing on $(y_b^+, +\infty)$.

With the above observations, we naturally obtain the monotonicity of the Poincaré map $\Phi(u)$ when the parameters meet different conditions as following three cases.

1) When $y_{d+1}^+ \leq y_b^+$, i.e., the maximum value of function $h(u)$ does not exceed y_b^+, then Φ increases monotonically on $[0, y_d^+)$ and decreases monotonically on $[y_d^+, +\infty)$, as shown in Fig. 3.2-(a);
2) When $y_b^+ \leq \tau$, i.e., the minimum value of function $h(u)$ is not less than y_b^+, then the monotonicity of map Φ is opposite to that of (1), as shown in Fig. 3.2-(b);
3) When $\tau < y_b^+ < y_{d+1}^+$ holds, then there is a trajectory Γ_1 and Γ_1 starting from point (EP_1, y_g^+) with $y_g^+ > y_d^+$ first intersects L_1 at point (EP_1, y_f^+) with $y_f^+ < y_d^+$ and then intersects L_3 at point (ET, y_b), where $y_b = (y_b^+ - \tau)/(1 - q_2)$. Obviously, $h(u) \in [\tau, y_b^+]$ for all $u \in [0, y_f^+] \cup [y_g^+, +\infty)$, while $h(u) \in (y_b^+, y_{d+1}^+]$ for all $u \in (y_f^+, y_g^+)$. Thus, combining the monotonicity of $h(u)$ and $G_2(u)$ and the range of $h(u)$, then $\Phi(u)$ is increasing on $[0, y_f^+) \cup [y_d^+, y_g^+)$ and decreasing on $[y_f^+, y_d^+) \cup [y_g^+, +\infty)$ with $\Phi(y_f^+) = \Phi(y_g^+)$, which means that Φ is a special bimodal map, as shown in Fig. 3.2-(c).

For concavity, note that under hypotheses (H2)' and (H8). We claim that Φ is concave down on interval D_0, where $D_0 = (0, y_d^+)$ for case 1) and $D_0 = (0, y_f^+)$ for case 3). That means we need to prove $\Phi''(u) < 0$ for all $u \in D_0$ in case 1) and case 3).

First, from the continuous differentiability of the solution of (2.1) with respect to the initial value, it can be obtained that functions $G_1(u)$ and $G_2(u)$ are second-order continuously differentiable. Further, since $\Phi(u) = (1 - q_1)G_2((1 - q_2)G_1(u) + \tau) + \tau$, the compound map Φ belongs to $C^2(R_+, R_+)$.

In range Ω, where

$$\Omega = \{(x, y)|0 \le y < \varphi_1(x), \ 0 < x < \min\{\bar{x}, \hat{x}\}\}, \tag{3.7}$$

model (2.1) can be rewritten as the following scalar differential equation

$$\frac{dy}{dx} = \frac{y F_2(x, y)}{x F_1(x, y)} = \frac{Q(x, y)}{P(x, y)} \dot{=} G(x, y). \tag{3.8}$$

The initial condition of (3.8) is $y(x_0) := u \in (0, y_d^+)$ when $x_0 = EP_1$ or $y(x_0) := u \in (0, y_b^+)$ when $x_0 = EP_2$. Notice that on Ω function $G(x, y)$ belongs to C^2 provided that conditions (H2)' holds.

The solution of (3.8) can be denoted as $y(x; x_0, u)$ and the partial derivative of solution $y(x; x_0, u)$ to the initial value u is as follows

$$y_u(x; x_0, u) = \exp\left(\int_{x_0}^{x} G_y(x, y(x; x_0, u))dx\right). \tag{3.9}$$

Hence, for function $G_1(u) = y(ET; EP_1, u)$ on interval $(0, y_d^+)$ or for function $G_2(u) = y(ET; EP_2, u)$ on $(0, y_b^+)$, there is

$$G_i'(u) = y_u(ET; EP_i, u) = \exp\left(\int_{EP_i}^{ET} G_y(x, y(x; EP_i, u))dx\right) > 0, \ i = 1, 2. \tag{3.10}$$

For (3.3), we have

$$\Phi'(u) = (1 - q_1)(1 - q_2)G_2'(h(u))G_1'(u)$$

$$= (1 - q_1)(1 - q_2)\exp\left(\int_{EP_2}^{ET} G_y(x, y(x; EP_2, h(u)))dx + \int_{EP_1}^{ET} G_y(x, y(x; EP_1, u))dx\right) \tag{3.11}$$

and

$$\Phi''(u) = \Phi'(u) \cdot \left[\left(\int_{EP_2}^{ET} G_{yy}(x, y(x; EP_2, h(u))) \cdot y_h(x; EP_2, h(u)) dx \right) (1 - q_2) G_1'(u) \right.$$

$$\left. + \left(\int_{EP_1}^{ET} G_{yy}(x, y(x; EP_1, u)) \cdot y_u(x; EP_1, u) dx \right) \right],$$

(3.12)

where

$$G_y(x, y) = \frac{F_2 + y F_{2y}}{x F_1} - \frac{y F_2 F_{1y}}{x (F_1)^2}$$

(3.13)

and

$$G_{yy}(x, y) = \frac{2 F_{2y} + y F_{2yy}}{x F_1} - \frac{y F_2 F_{1yy}}{x (F_1)^2} - \frac{2 F_{1y}(F_2 + y F_{2y})}{x (F_1)^2} + \frac{2 y F_2 (F_{1y})^2}{x (F_1)^3}.$$

(3.14)

Note that when (H8) holds, $F_{1yy} = 0$ and $F_{2yy} = 0$, then (3.14) can be simplified as

$$G_{yy}(x, y) = \frac{2 F_{2y}}{x F_1} - \frac{2 F_{1y}(F_2 + y F_{2y})}{x (F_1)^2} + \frac{2 y F_2 (F_{1y})^2}{x (F_1)^3},$$

(3.15)

which is less than zero on range Ω, since condition (H5) holds, $F_1 > 0$ and $F_2 < 0$ on Ω, as shown in Fig. 2.1. For (3.12), combining $G_{yy}(x, y) < 0$ on Ω with $\Phi'(u) > 0$, $y_h(x; EP_2, h(u)) > 0$, $y_u(x; EP_1, u) > 0$, and $(1 - q_2) G_1'(u) > 0$ for all $u \in D_0$, there is $\Phi''(u) < 0$ for all $u \in D_0$ for case 1) and case 3).

Horizontal Asymptote. For continuous function $G_1(u)$, which is monotonically decreasing on $[y_d^+, +\infty)$ and $G_1(u) \in [0, y_{d+1}]$, we claim that $\lim_{u \to +\infty} G_1(u) = 0$. Otherwise, there exists a positive y_* satisfying $\lim_{u \to +\infty} G_1(u) = y_*$. Choose an arbitrary point (ET, y_1) on phase curve L_3 with $0 < y_1 < y_*$. It follows from the uniqueness of a solution to ordinary differential equation (2.1) that there must exist a point (EP_1, y_0^+) on L_1 such that $G_1(y_0^+) = y_1$ with $y_0^+ \geq +\infty$, which is a contradiction. Thus,

$$\lim_{u \to +\infty} G_1(u) = 0 = G_1(0).$$

(3.16)

For continuous function $G_2(u)$, there is $\lim_{u \to \tau} G_2(u) = G_2(\tau)$. Thus, we naturally obtain that the limit of continuous compound function (3.3) is as follows:

$$\lim_{u \to +\infty} (1 - q_1) G_2 ((1 - q_2) G_1(u) + \tau) + \tau = (1 - q_1) G_2(\tau) + \tau,$$

(3.17)

that is, $\lim_{u \to +\infty} \Phi(u) = \Phi(0)$, which indicates that line $y = \Phi(0)$ is the horizontal asymptote of the map Φ, as shown in Fig. 3.2. This completes the proof. $\quad\square$

Theorem 3.2 discusses the existence and the global stability of fixed point of map Φ when $\tau = 0$.

Theorem 3.2. *Assume $ET < \min\{\bar{x}, \hat{x}\}$ and (S1) is applied. When $\tau = 0$, the map Φ has a unique trivial fixed point, which is globally stable. This means that impulsive model (2.2)-(2.4) has a globally stable predator-free periodic solution (PFPS).*

Proof. When $\tau = 0$, it is obvious that $\Phi(0) = 0$. Because $dy/dt = yF_2(x, y) < 0$ in area $\{(x, y) | 0 < x < \min\{\bar{x}, \hat{x}\}, y > 0\}$, as shown in Fig. 2.1, there are $G_1(u) < u$ and $G_2(u) < u$ for all $u > 0$, where

$$G_1(u) := y(ET; x_0 = EP_1, y_0 = u), \quad G_2(u) := y(ET; x_0 = EP_2, y_0 = u),$$

are defined by the solutions of model (3.8) with $ET < \min\{\bar{x}, \hat{x}\}$. From the above, there is

$$\Phi(u) = (1 - q_1)G_2((1 - q_2)G_1(u)) < (1 - q_1)(1 - q_2)G_1(u) < u \Rightarrow$$
$$\Phi(u) < u \text{ for all } u > 0. \tag{3.18}$$

Thus, we have proved that $u^* = 0$ is the unique fixed point of map $\Phi(u)$.

It follows from the assumptions (H3) and (H4) that $G_y(x, 0) = F_2(x, 0)/[xF_1(x, 0)] < 0$ for all $x < ET < \min\{\bar{x}, \hat{x}\}$, which indicates that for (3.11), there is

$$0 < \Phi'(0) = (1 - q_1)(1 - q_2) \exp \left(\int_{EP_2}^{ET} G_y(x, 0)dx + \int_{EP_1}^{ET} G_y(x, 0)dx \right) < 1. \tag{3.19}$$

It is known that for the one-dimensional discrete mapping $\Phi(u)$ with $|\Phi'(0)| < 1$, the trivial fixed point is locally asymptotically stable.

Finally, we prove that the trivial fixed point is globally attractive. Because $\Phi(u) < u$ for all $u > 0$ as shown in (3.18), there is

$$0 \leq \cdots < \Phi^n(u) < \Phi^{n-1}(u) < \cdots < \Phi(u) < u \text{ for all } u > 0 \text{ and } n \geq 1. \tag{3.20}$$

Hence, point column $\{\Phi^n(u)\}$ is monotonically decreasing and $\lim_{n \to +\infty} \Phi^n(u) = 0$ for all $u \geq 0$. Otherwise, if $\lim_{n \to +\infty} \Phi^n(u) = \tilde{y} > 0$ then there is $\Phi(\tilde{y}) < \tilde{y}$, which is a contradiction. This completes the proof. $\square$

Obviously, when the releasing number of predators is greater than zero, i.e., $\tau > 0$, Φ does not have trivial fixed point. In the following theorem, we discuss the number of positive fixed points of Φ corresponding to the number of positive periodic solutions of the impulsive model (2.2)-(2.4).

Theorem 3.3. *Assume $ET < \min\{\bar{x}, \hat{x}\}$ and (S1) is applied. When $\tau > 0$, the Poincaré map $\Phi(u)$ may be unimodal, inverted U-shaped, or bimodal. Further,*

(i) $\Phi(u)$ *has at least one positive fixed point.*

(ii) *there is at most one fixed point in each monotonically decreasing subinterval.*
(iii) *the number of fixed points of the map $\Phi(u)$ depends on the number of fixed points of $\Phi(u)$ in monotonically increasing interval.*

Proof. When $\tau > 0$, the relationship between τ, y_{d+1}^+, and y_b^+ can be one of the three cases: $y_{d+1}^+ \le y_b^+$, or $y_b^+ \le \tau$, or $\tau < y_b^+ < y_{d+1}^+$. Thus, the monotonicity of the continuous map $\Phi(u)$ is shown in Theorem 3.1, and the shape of $\Phi(u)$ may be unimodal, inverted U-shaped, or bimodal, as shown in Fig. 3.2.

(i) Obviously, $\Phi(0) = (1 - q_1)G_2(\tau) + \tau > 0$. For the continuous and bounded map Φ, there exists a large enough u_0 to make $\Phi(u_0) < u_0$. Hence, the map Φ has at least one positive fixed point.

(ii) First, we claim that the fixed point may be in the decreasing interval of $\Phi(u)$. According to the intermediate value theorem of continuous function $\Phi(u)$, the sufficient conditions for the existence of positive fixed points u^* in the monotonically decreasing subinterval of map $\Phi(u)$ are as follows:

- when $y_{d+1}^+ \le y_b^+$, then there exists a fixed point $u^* \in (y_d^+, +\infty)$ if $\Phi(y_d^+) > y_d^+$;
- when $y_b^+ \le \tau$, then there exists a fixed point $u^* \in (0, y_d^+)$ if $\Phi(y_d^+) < y_d^+$;
- when $\tau < y_b^+ < y_{d+1}^+$, then there is a fixed point $u^* \in (y_f^+, y_d^+)$ if $\Phi(y_f^+) > y_f^+$ and $\Phi(y_d^+) < y_d^+$, and fixed point $u^* \in (y_g^+, +\infty)$ if $\Phi(y_g^+) > y_g^+$.

Next, we prove that on the monotonically decreasing subinterval of map $\Phi(u)$, the number of fixed point does not exceed 1. Take the last case (i.e., $\tau < y_b^+ < y_{d+1}^+$ and $\Phi(u)$ is a bimodal map) as an example. If there are at least two positive fixed points on decreasing subinterval (y_f^+, y_d^+), let us assume that two of them are u_1^* and u_2^* with $y_f^+ < u_1^* < u_2^* < y_d^+$, then $u_1^* = \Phi(u_1^*) > \Phi(u_2^*) = u_2^*$, which is a contradiction.

(iii) The number of fixed points of map $\Phi(u)$ on monotonically decreasing interval is finite, which have proved in (ii). However, on the increasing interval of $\Phi(u)$, the convexity of Φ is complex and possibly changeable, which has a great influence on the number of fixed points. This completes the proof. □

From the proof of the above theorem together with the fact that $\Phi(y_g^+) > y_g^+$ implies $\Phi(y_f^+) > y_f^+$, we actually have the following corollary.

Corollary 3.1. *Assume $ET < \min\{\bar{x}, \hat{x}\}$ and (S1) is applied. When $0 < \tau < y_b^+ < y_{d+1}^+$, the map $\Phi(u)$ has at least three fixed points (i.e., model (2.2)-(2.4) has at least three positive periodic solutions) provided that $\Phi(y_d^+) < y_d^+$ and $\Phi(y_g^+) > y_g^+$.*

Theorems 3.4 and 3.5 give the sufficient condition for the stability of the positive fixed point of Poincaré map Φ. Passing these condition to the impulsive model (2.2)-(2.4), the following two theorems discuss the sufficient condition for the stability of the positive periodic solution of impulsive model (2.2)-(2.4).

Theorem 3.4. *Assume $ET < \min\{\bar{x}, \hat{x}\}$ and (S1) is applied. When $\tau > 0$, $y_{d+1}^+ \le y_b^+$, $\Phi(y_d^+) < y_d^+$, (H2)' and (H8) hold, then $\Phi(u)$ has a unique fixed point $u^* \in (0, y_d^+)$, which is globally stable.*

Proof. It follows from $\Phi(0) > 0$ and $\Phi(y_d^+) < y_d^+$ that there exists a $u^* \in (0, y_d^+)$ satisfying $\Phi(u^*) = u^*$. The fixed point u^* is unique, because $\Phi(u)$ is concave down and increasing on interval $(0, y_d^+)$, as shown in Theorem 3.1(ii), and meanwhile, there is no fixed point on decreasing interval $[y_d^+, +\infty)$ since $u \geq y_d^+ > \Phi(y_d^+) \geq \Phi(u)$ for all $u > y_d^+$.

Now, we prove that the unique fixed point u^* is globally stable.

- For $u \in (0, u^*)$, it follows from $u < \Phi(u) < u^*$ that

$$u < \Phi(u) < \cdots < \Phi^{n-1}(u) < \Phi^n(u) < u^*,$$

which indicates that $\Phi^n(u)$ increases monotonically toward u^* as $n \to +\infty$.

- For $u \in (u^*, +\infty)$, when $\Phi(u) < u^*$, then similar to above case, $\lim_{n\to+\infty} \Phi^n(u) = u^*$. However, when $\Phi(u) > u^*$, since $\Phi(u) < \Phi(y_d^+) < y_d^+$, $\Phi[u^*, y_d^+] \subseteq [u^*, \Phi(y_d^+)] \subset [u^*, y_d^+]$, and $\Phi(\bar{u}) < \bar{u}$ for all $u^* < \bar{u}$, then

$$u^* < \Phi^n(u) < \Phi^{n-1}(u) < \cdots < \Phi(u) < y_d^+,$$

that is, $\Phi^n(u)$ decreases monotonically toward u^* as $n \to +\infty$. This completes the proof. $\square$

Theorem 3.5. *Assume $ET < \min\{\bar{x}, \hat{x}\}$ and (S1) is applied. When $\tau > 0$, $y_{d+1}^+ \leq y_b^+$, $\Phi(y_d^+) > y_d^+$, (H2)' and (H8) hold, then the map Φ has a unique fixed point $u^* \in (y_d^+, +\infty)$, as shown in Fig. 3.2-(a). Further,*

(i) *if $\Phi^2(u) > u$ for all $u \in [y_d^+, u^*)$, then u^* is globally stable.*

(ii) *if $\Phi^2(y_d^+) \geq y_d^+$, then Φ has a globally stable fixed point on $(y_d^+, +\infty)$ or a two-point cycle coexisting with the fixed point such that any other trajectory of system (2.2)-(2.4) will approach either an order-1 periodic solution or an order-2 periodic solution as $t \to \infty$.*

(iii) *if $\Phi^2(y_d^+) < y_d^+$, where $y_{v_1}^+ = \min\{u | \Phi(u) = y_d^+\}$, then Φ has a periodic point with period k ($k = 1, 2, 3, \ldots$), i.e., (2.2)-(2.4) has order-k periodic solutions.*

The proof process of Theorem 3.5 is similar to that of Theorems 5, 6 and 7 in Ref. [35] but is a bit lengthy. For integrity of this article, we give the proof in Appendix A.

The following theorem discusses the stability of the fixed point of map Φ when Φ is inverted U-shaped.

Theorem 3.6. *Assume $ET < \min\{\bar{x}, \hat{x}\}$, (S1) is applied, and $y_b^+ \leq \tau$.*

(i) *If $\Phi(0) \leq y_d^+$, then the Poincaré map Φ has a unique fixed point $u^* \in (0, y_d^+)$, which either is globally stable or coexists with 2-periodic points.*

(ii) *If $\Phi(0) \leq y_d^+$ and $\Phi^2(u) > u$ for all $u \in [0, u^*)$, u^* is globally stable.*

(iii) *If $\Phi(y_d^+) \geq y_d^+$ and Φ has a unique fixed point $u^* \in [y_d^+, +\infty)$ (see Fig. 3.2-(b)), then u^* is globally stable.*

Proof. Theorem 3.1 tells us that when the assumptions of Theorem 3.6 hold, function $\Phi(u)$ decreases on $[0, y_d^+)$ and increases on $(y_d^+, +\infty)$, moreover, $\lim_{u\to+\infty} \Phi(u) = \Phi(0)$.

(i) According to $\Phi(0)$ is the maximum value of function $\Phi(u)$, there is $\Phi(u) < \Phi(0) \leq y_d^+$ for any $y_d^+ \leq u$, which implies that there is no fixed point of Φ on interval $[y_d^+, +\infty)$. For continuous function Φ, there are $\Phi(0) > 0$ and $\Phi(y_d^+) < \Phi(0) \leq y_d^+$. Thus, the map Φ has a fixed point $u^* \in (0, y_d^+)$. Moreover, Theorem 3.3 (ii) guarantees that u^* is the unique fixed point.

It follows from $\Phi[0, +\infty) = [\Phi(y_d^+), \Phi(0)] \subset [0, \Phi(0)]$ that $\Phi^n(u) \in [0, \Phi(0)]$ for all $u \geq 0$. Therefore, we only need to analyze the property of $\{\Phi^n(u)\}$ when $u \in [0, \Phi(0)]$.

Denote

$$u_n = \Phi^n(u), \ (A_a): \lim_{k \to +\infty} u_{2k} \neq \lim_{k \to +\infty} u_{2k+1}, \ (A_b): \lim_{k \to +\infty} u_{2k} = \lim_{k \to +\infty} u_{2k+1} = u^*. \quad (3.21)$$

Because $\Phi(u)$ is decreasing on $[0, y_d^+] \supseteq [0, \Phi(0)]$ and $u^* < \Phi(0)$, there are $u^* < \Phi(u) < \Phi(0)$ for all $u < u^*$ and $0 < \Phi(u) < u^*$ for all $u^* < u < \Phi(0)$. Thus, when $u \in [0, \Phi(0)]$, we have the following four cases:

(a.1) $0 \leq u < u_2 < u_4 < u^* < u_3 < u_1 \leq \Phi(0) \Rightarrow (A_a)$ holds or (A_b) holds;
(a.2) $0 < u_4 < u_2 < u < u^* < u_1 < u_3 < \Phi(0) \Rightarrow (A_a)$ holds;
(a.3) $0 < u_3 < u_1 < u^* < u < u_2 < u_4 < \Phi(0) \Rightarrow (A_a)$ holds;
(a.4) $0 < u_1 < u_3 < u^* < u_4 < u_2 < u \leq \Phi(0) \Rightarrow (A_a)$ holds or (A_b) holds.

Therefore, (i) is proved.

(ii) According to the proof of above, Φ has no periodic point with period-n where $n \geq 3$, except a fixed point or periodic points with period-2. Suppose there are periodic points u_a and u_b with period-2, where $u_a < u_b$, $\Phi(u_a) = u_b$ and $\Phi^2(u_a) = u_a$. Cases (a.1)-(a.4) tell us that $0 < u_a < u^* < u_b < \Phi(0)$. However, $\Phi^2(u_a) = u_a < u^*$, which contradicts $\Phi^2(u) > u$ for all $u < u^*$. Hence, map Φ has no periodic point with period-2 and the unique fixed point u^* is globally stable.

(iii) From the assumption of (iii), it is easy to know that $u^* \in [y_d^+, +\infty)$ is the unique fixed point of map Φ, as shown in Fig. 3.2-(b). Further, $\Phi[0, +\infty) = [\Phi(y_d^+), \Phi(0)] \subset [y_d^+, +\infty)$, for any $y_d^+ < u < u^*$ there is $u < \Phi(u) < u^*$, and for any $u > u^*$ there is $u > \Phi(u) > u^*$. Hence, for any $u \geq 0$, $\Phi^n(u)$ increases (or decreases) toward u^* as $n \to +\infty$. □

Theorems 3.2, 3.4, 3.5 and 3.6 discussed the existence and stability of the fixed point only when $\Phi(u)$ has a single extremal point. In the following Theorems 3.7, 3.8 and 3.9, we investigate the properties of Φ when Φ has two maximum points [11,7,18]. As a preparation, we first note that according to Theorem 3.1, under the assumptions of $0 < \tau < y_b^+ < y_{d+1}^+$, (H2)' and (H8), map Φ is a special bimodal map, which is monotonically increasing and concave down on $(0, y_f^+)$, decreasing on $(y_f^+, y_d^+) \cup (y_g^+, +\infty)$, and increasing on (y_d^+, y_g^+). Further,

$$\Phi(y_f^+) = \Phi(y_g^+) > \Phi(u) \text{ for all } u \in [0, +\infty) \setminus \{y_f^+, y_g^+\} \quad (3.22)$$

and

$$\lim_{u \to +\infty} \Phi(u) = \Phi(0). \quad (3.23)$$

Theorem 3.7. *Assume $ET < \min\{\bar{x}, \hat{x}\}$ and (S1) is applied. When $0 < \tau < y_b^+ < y_{d+1}^+$, (H2)' and (H8) hold, then the map Φ has the following properties.*

(i) If $\Phi(y_f^+) < y_f^+$, Φ has a unique and globally stable fixed point $u^* \in (0, y_f^+)$.

(ii) If $\Phi(y_d^+) > y_d^+$ and $\Phi(y_g^+) < y_g^+$, Φ has at least one fixed point u^* and u^* must belong to (y_d^+, y_g^+).

(iii) If there is a unique $u^* \in (y_d^+, y_g^+)$ such that $\Phi(u^*) = u^*$, $\Phi(u) > u$ for all $u \in [y_d^+, u^*)$, and $\Phi(u) < u$ for all $u \in (u^*, y_g^+]$, then u^* is the unique and globally stable fixed point of Φ.

Proof. (i) The proof process of (i) is similar to that of Theorem 3.4. $\Phi(0) > 0$ is obvious. If $\Phi(y_f^+) < y_f^+$ holds, one yields that there exists a $u^* \in (0, y_f^+)$ satisfying $\Phi(u^*) = u^*$. The concavity of Φ tells us that u^* is the unique fixed point of Φ on $(0, y_f^+)$. Moreover, it follows from the monotonicity of $\Phi(u)$ that $\Phi(u) \le \Phi(y_f^+) < y_f^+$ for all $u > y_f^+$, i.e., $\Phi(u) < u$ for all $u > y_f^+$. Thus, u^* is the unique fixed point of Φ.

From $\Phi[0, +\infty) \subset [0, \Phi(y_f^+)] \subset [0, y_f^+]$, $u < \Phi(u) < u^*$ for all $u \in [0, u^*)$, and $u^* < \Phi(u) < u$ for all $u \in (u^*, y_f^+]$. It follows that $\Phi^n(u)$ is monotonically increasing to u^* for any $u \in [0, u^*)$, and $\Phi^n(u)$ is monotonically decreasing to u^* for any $u \in (u^*, y_f^+]$. Hence, for any $u \in [0, +\infty)$, $\{\Phi^n(u)\}$ converges to u^*.

(ii) When $\Phi(y_d^+) > y_d^+$ and $\Phi(y_g^+) < y_g^+$, then map Φ has at least one fixed point u^* on (y_d^+, y_g^+) according to the intermediate value theorem of continuous function. In the following, we prove that on $[0, y_d^+] \cup [y_g^+, +\infty]$ map Φ has no fixed point.

- For all $u \in [y_g^+, +\infty)$, $\Phi(u)$ is decreasing. There is $\Phi(u) \le \Phi(y_g^+) < y_g^+ \le u$, which means $\Phi(u) < u$ for all $u \ge y_g^+$;
- For all $u \in [y_f^+, y_d^+]$, $\Phi(u)$ is still decreasing. There is $\Phi(u) \ge \Phi(y_d^+) > y_d^+ \ge u$, which means $\Phi(u) > u$ for all $u \in [y_f^+, y_d^+]$ and thus $\Phi(y_f^+) > y_f^+$;
- It follows from $\Phi(u)$ is increasing and concave down on $[0, y_f^+]$, $\Phi(0) > 0$, and $\Phi(y_f^+) > y_f^+$, that $\Phi(u) > u$ for all $u \in [0, y_f^+]$.

Hence, $\Phi(u) \ne u$ for all $u \in [0, y_d^+] \cup [y_g^+, +\infty]$.

(iii) Hypothesis $\Phi(u) > u$ for all $u \in [y_d^+, u^*)$ tells us that $\Phi(y_d^+) > y_d^+$, and hypothesis $\Phi(u) < u$ for all $u \in (u^*, y_g^+]$ implies that $\Phi(y_g^+) < y_g^+$. Therefore, combining the proof of (ii) and the assumptions of (iii), we can obtain that $\Phi(u) > u$ for all $u < u^*$ and $\Phi(u) < u$ for all $u > u^*$, that is, u^* is the unique fixed point of Φ.

Finally, we claim that u^* is globally stable, that is, $\{\Phi^n(u)\}$ converges to u^* for any $u \in [0, +\infty)$. It is noted that $\Phi(u)$ is increasing on $(0, y_f^+) \cup (y_d^+, u^*)$ and decreasing on (y_f^+, y_d^+). The maximum value $\Phi(y_f^+)$ of Φ belongs to (u^*, y_g^+) since $\Phi(y_f^+) = \Phi(y_g^+) < y_g^+$ and $\Phi(u)$ increases on (u^*, y_g^+). Denote $Y_* = \{u | \Phi(u) = u^*, y_f^+ < u < y_d^+\}$. We discuss the convergence of $\{\Phi^n(u)\}$ when $u \in [0, y_f^+]$, $u \in [y_f^+, Y_*)$, $u \in (Y_*, u^*)$, $u \in (u^*, \Phi(y_f^+)]$, or $u \in (\Phi(y_f^+), +\infty)$ as follows.

1) For all $u \in (Y_*, u^*)$, $\Phi(u) \in [\Phi(y_d^+), u^*) \subset [y_d^+, u^*)$ and $\bar{u} < \Phi(\bar{u})$ for all $\bar{u} \in [y_d^+, u^*)$. Thus, $\Phi^n(u)$ is monotonically increasing toward u^* as $n \to +\infty$;

2) For all $u \in (u^*, \Phi(y_f^+)]$, $\Phi(u) < u$ and $\Phi(u)$ is increasing. Thus, there is $u^* < \cdots < \Phi^2(u) < \Phi(u) < u \le \Phi(y_f^+)$, which indicates that $\Phi^n(u)$ is monotonically decreasing toward u^* as $n \to +\infty$;

3) For all $u \in [y_f^+, Y_*)$, $\Phi(u) \in (u^*, \Phi(y_f^+)]$. Similar to 2), $\lim_{n\to+\infty} \Phi^n(u) = u^*$;

4) For all $u \in [0, y_f^+]$, $\Phi(u) > u$ and $\Phi(u)$ is increasing. Thus, there exists a $k \ge 1$ such that $\Phi^{(k)}(u) \in [y_f^+, \Phi(y_f^+)]$. Similar to 1)-3), $\lim_{n\to+\infty} \Phi^n(u) = u^*$;

5) For all $u \in (\Phi(y_f^+), +\infty)$, $\Phi(u) \in [\Phi(0), \Phi(y_f^+)] \subset [0, \Phi(y_f^+)]$. Thus, similar to 1)-4), $\lim_{n\to+\infty} \Phi^n(u) = u^*$. □

The following corollary can be drawn from Theorem 3.4, Theorem 3.6(iii), and Theorem 3.7.

Corollary 3.2. *Assume $ET < \min\{\bar{x}, \hat{x}\}$ and (S1) is applied. When $\tau > 0$, map $\Phi(u)$ has a unique fixed point u^*, and u^* belongs to the increasing interval of Φ, then u^* is globally stable.*

Theorem 3.8. *Assume $ET < \min\{\bar{x}, \hat{x}\}$, (S1) is applied, $0 < \tau < y_b^+ < y_{d+1}^+$, and Φ has a unique fixed point $u^* > y_g^+$, as shown in Fig. 3.2-(c).*

(i) *If $\Phi^2(u) > u$ for all $u \in [y_g^+, u^*)$, then u^* is globally stable.*

(ii) *If $\Phi^2(y_g^+) \ge y_g^+$, then u^* is globally stable or Φ has a two-point cycle coexisting with the fixed point.*

(iii) *If $\Phi^2(y_g^+) < y_{v_2}^+$, where $y_{v_2}^+ = \min\{u| \Phi(u) = y_g^+\}$, then Φ has a periodic point with period k ($k = 1, 2, 3, \ldots$), i.e., (2.2)-(2.4) has order-k periodic solutions.*

Proof. Under the assumptions of Theorem 3.8, it follows from Theorem 3.1(iv) that Φ is a special bimodal map, as shown in Fig. 3.2-(c). Moreover, because u^* is the unique fixed point of Φ, there are $\Phi(u) > u$ for all $u < u^*$ and $\Phi(u) < u^*$ for all $u^* < u$.

(i) Under the assumption of $\Phi^2(u) > u$ for any $u \in [y_g^+, u^*)$, we prove $\lim_{n\to+\infty} u_n = u^*$ in the following three cases, where $u_n := \Phi^n(u)$.

- For all $u \in [y_g^+, u^*)$, because $\Phi(u)$ is decreasing on $[y_g^+, +\infty)$ and $\bar{u} < \Phi^2(\bar{u})$ when $\bar{u} \in [y_g^+, u^*)$, there is $y_g^+ \le u < u_2 < u_4 < \cdots < u^* < \cdots < u_3 < u_1$. By analogy, u_{2k} is monotonically increasing to u^* and u_{2k+1} is monotonically decreasing to u^*. Hence, $\lim_{n\to+\infty} u_n = u^*$;

- For all $u \in X_1 := \{u|u \ge 0, \Phi(u) > u^*\} \setminus [y_g^+, u^*)$, there is $u^* < \Phi(u) \le \Phi(y_g^+)$. Since $\Phi[y_g^+, u^*) = (u^*, \Phi(y_g^+)]$, there exists a $\hat{u}_1 \in [y_g^+, u^*)$ such that $\Phi(\hat{u}_1) = \Phi(u)$. Thus, the situation reduces to the above case and $\lim_{n\to+\infty} u_n = u^*$ also holds true;

- For all $u \in X_2 := \{u|u \ge 0, \Phi(u) < u^*\}$, there must exist an m and a $\hat{u}_2 \in [y_g^+, u^*) \cup X_1$ such that $\Phi^m(u) = \Phi(\hat{u}_2) > u^*$ or $\Phi^m(u) = u^*$, which implies that the situation again reduces to the above two cases and $\lim_{n\to+\infty} u_n = u^*$.

(ii) According to the above analysis process, we only need to know the properties of point sequence $\{u_n\}$ when $u \in [y_g^+, u^*)$ to judge the stability of the fixed point of map Φ.

When $u \in [y_g^+, u^*)$, it follows from $\Phi(u)$ is decreasing on $[y_g^+, +\infty)$ and $\Phi^2(y_g^+) \ge y_g^+$ that $\Phi(y_g^+) > \Phi(u) > \Phi(u^*) = u^* > y_g^+$ and $y_g^+ \le \Phi^2(y_g^+) \le \Phi^2(u) < u^*$, that is,

$$y_g^+ \le u < u^* < u_1 < \Phi(y_g^+), \ y_g^+ \le u_2 < u^*. \tag{3.24}$$

According to (3.24), there are the following three possible situations:

1) $u = u_2 \ne u_1$;
2) $u_2 < u \Rightarrow y_g^+ \le u_4 < u_2 < u < u^* < u_1 < u_3 < \Phi(y_g^+) \Rightarrow \lim_{k\to+\infty} u_{2k} \ne \lim_{k\to+\infty} u_{2k+1}$;
3) $u < u_2 \Rightarrow y_g^+ \le u < u_2 < u_4 < u^* < u_3 < u_1 < \Phi(y_g^+) \Rightarrow \lim_{k\to+\infty} u_{2k} \ne \lim_{k\to+\infty} u_{2k+1}$
   or $\lim_{k\to+\infty} u_{2k} = \lim_{k\to+\infty} u_{2k+1} = u^*$.

Therefore, if and only if 3) occurs and $\lim_{k\to+\infty} u_{2k} = \lim_{k\to+\infty} u_{2k+1}$ for all $u \in [y_g^+, u^*)$, then the fixed point u^* is globally stable. On the contrary, two-point cycles coexist with the unique fixed point.

(iii) The proof of (iii) is the same as the proof of Theorem 3.5(iii). □

Theorem 3.9. *Assume $ET < \min\{\bar{x}, \hat{x}\}$ and (S1) is applied. When $0 < \tau < y_b^+ < y_{d+1}^+$, Φ has a unique fixed point $u^* \in (y_f^+, y_d^+)$ and $\Phi^2(u) > u$ for all $u \in [y_f^+, u^*)$, then u^* is globally stable.*

The proof of Theorem 3.9 is similar to that of Theorem 1 in Ref. [27], for convenience, we put the proof in Appendix B.

4. The existence and stability of PFPS and its bifurcation

4.1. The existence and stability of PFPS

Assume $\tau = 0$, $ET < \bar{x}$, and strategy (S1) is applied for impulsive system (2.2)-(2.4). When $y_0 = 0$, there is $y(t) \equiv 0$ for all $t \ge 0$ and (2.2)-(2.4) can be simplified as follows:

$$\begin{cases} dx(t)/dt = x(t)F_1(x(t), 0), & \text{if } x(t) = ET, \\ x(t^+) = (1 - p_2)x(t), & \text{if } x(t) = ET, \ j = 2n - 1, \\ x(t^+) = (1 - p_1)x(t), & \text{if } x(t) = ET, \ j = 2n, \ n \ge 1, \end{cases} \tag{4.1}$$

where t_j represents the time of the j-th pulse happened.

For model (4.1), since $\dot{x}(t) > 0$ for all $x < ET$ with $ET < \bar{x}$, the trajectory starting from $x_0 = (1 - p_1)ET = EP_1$ reaches pulse line $x = ET$ after a finite time T_1, then pulses to phase line $x = (1 - p_2)ET = EP_2$, and then reaches pulse line $x = ET$ again after a finite time T_2, where T_i (i=1, 2) satisfies the following integral equation

$$\int_{EP_i}^{ET} \frac{dx}{xF_1(x, 0)} dx = T_i. \tag{4.2}$$

Denote $T = T_1 + T_2$.

According to the above analysis, we find that system (4.1) has a periodic solution $\xi(t)$ with period T, which satisfies $\xi(0^+) = EP_1$, $\xi(T_1) = ET$, $\xi(T_1^+) = EP_2$, $\xi(T) = ET$, and $\xi(T^+) = EP_1$. Further, $\xi(t)$ also satisfies the following equations

$$
\begin{cases}
\displaystyle\int_{EP_1}^{\xi(t)} \frac{dx}{x F_1(x,0)} = t - nT, \ \text{for } t \in [nT^+, nT + T_1], \\[1em]
\displaystyle\int_{EP_2}^{\xi(t)} \frac{dx}{x F_1(x,0)} = t - (nT + T_1), \ \text{for } t \in [(nT + T_1)^+, (n+1)T], \ n \geq 0.
\end{cases}
\tag{4.3}
$$

Note that $(\xi(t), 0)$ is a PFPS of the impulsive model (2.2)-(2.4) when strategy (S1) is applied.

According to Lemma 2.3, we can obtain the sufficient condition for local stability of the periodic solution of model (2.2)-(2.4), which is shown in Theorem 4.1.

Theorem 4.1. *Assume $ET < \bar{x}$ and (S1) is applied. When $\tau = 0$ and (4.9) hold, then the T-periodic solution $(\xi(t), 0)$ of system (2.2)-(2.4) is orbitally asymptotically stable.*

Proof. Lemma 2.3 tells us that if the modulus of Floquet multiplier μ_2 is less than 1 where

$$
\mu_2 = \triangle_1 \cdot \triangle_2 \exp\left[\int_0^T P_x(\xi(t), 0)dt\right] \exp\left[\int_0^T Q_y(\xi(t), 0)dt\right],
\tag{4.4}
$$

the PFPS $(\xi(t), 0)$ is orbitally asymptotically stable.

First of all, when $\tau = 0$ and strategy (S1) is used for model (2.2)-(2.4), the formula $\triangle_1$ and $\triangle_2$ related to the periodic solution $(\xi(t), 0)$ are shown in (2.7), where $\phi(x, y) = x - ET$, $a_1(x, y) = -p_2 x$, $b_1(x, y) = -q_2 y$, $a_2(x, y) = -p_1 x$, $b_2(x, y) = -q_1 y$, $\xi(T_1) = \xi(T) = ET$, $\xi(T_1^+) = EP_2$, and $\xi(T^+) = EP_1$. Therefore, there are

$$
\triangle_1 = (1 - q_2)\frac{P(\xi(T_1^+), 0)}{P(\xi(T_1), 0)} = (1 - q_2)\frac{P(EP_2, 0)}{P(ET, 0)}
\tag{4.5}
$$

and

$$
\triangle_2 = (1 - q_1)\frac{P(\xi(T^+), 0)}{P(\xi(T), 0)} = (1 - q_1)\frac{P(EP_1, 0)}{P(ET, 0)}.
\tag{4.6}
$$

Next, taking the transformation $dt = dx/\dot{x}$ in expression $\exp\left[\int_0^T P_x(\xi(t), 0)dt\right]$ yields

$$
\exp\left(\int_0^T P_x(\xi(t), 0)dt\right)
$$

$$
= \exp\left(\int_0^{T_1} P_x(\xi(t), 0)dt + \int_{T_1^+}^T P_x(\xi(t), 0)dt\right)
$$

$$= \exp\left(\int_{EP_1}^{ET} \frac{P_x(x,0)}{P(x,0)}dx + \int_{EP_2}^{ET} \frac{P_x(x,0)}{P(x,0)}dx\right)$$

$$= \exp\left[\ln\left(\frac{P(ET,0)}{P(EP_1,0)}\right) + \ln\left(\frac{P(ET,0)}{P(EP_2,0)}\right)\right] = \frac{P(ET,0)}{P(EP_1,0)}\frac{P(ET,0)}{P(EP_2,0)}. \tag{4.7}$$

Combining (4.5), (4.6) and (4.7), we obtain $\Delta_1\Delta_2 \exp\left(\int_0^T P_x(\xi(t),0)dt\right) = (1-q_1)(1-q_2)$. Hence, the value of Floquet multiplier μ_2 in (4.4) as the following

$$\mu_2 = (1-q_1)(1-q_2)\exp\left(\int_0^{T_1} Q_y(\xi(t),0)dt + \int_{T_1^+}^{T} Q_y(\xi(t),0)dt\right)$$

$$= (1-q_1)(1-q_2)\exp\left(\int_{EP_1}^{ET} \frac{Q_y(x,0)}{P(x,0)}dx + \int_{EP_2}^{ET} \frac{Q_y(x,0)}{P(x,0)}dx\right), \tag{4.8}$$

where $Q_y(x,0)/P(x,0) = F_2(x,0)/[xF_1(x,0)]$.

Therefore, if

$$\mu_2 = (1-q_1)(1-q_2)\exp\left(\int_{EP_2}^{ET}\left(\frac{F_2(x,0)}{xF_1(x,0)}\right)dx + \int_{EP_1}^{ET}\left(\frac{F_2(x,0)}{xF_1(x,0)}\right)dx\right) < 1, \tag{4.9}$$

then $|\mu_2| < 1$ and the PFPS $(\xi(t),0)$ is orbitally asymptotically stable. $\quad\square$

Combining the above proof process and the basic assumptions (H3) and (H4) on the population growth rate function, we have the following results.

Theorem 4.2. *Assume $ET < \bar{x}$ and (S1) is applied for (2.2)-(2.4). When $\tau = 0$, $q_1 = q_2 = 0$, $EP_1 > \hat{x}$, and $EP_2 > \hat{x}$ hold, the periodic solution $(\xi(t),0)$ is unstable.*

Proof. As shown in assumptions (H3) and (H4), there exists $\bar{x} > 0$ and $\hat{x} > 0$ such that $F_1(x,0) > 0$ for all $0 < x < \bar{x}$ and $F_2(x,0) > 0$ for all $x > \hat{x}$. Thus, if $ET < \bar{x}$, $EP_1 > \hat{x}$, and $EP_2 > \hat{x}$ then $F_2(x,0)/[xF_1(x,0)] > 0$ holds for all $x \in (EP_1, ET)$ or $x \in (EP_2, ET)$, that is, $\mu_2 > 1$ and $(\xi(t),0)$ is unstable. This completes the proof. $\quad\square$

Remark 4.1. If $ET < \min\{\bar{x},\hat{x}\}$, then $F_2(x,0)/[xF_1(x,0)] < 0$ for $x \in (0, ET)$, which implies the value of Floquet multiplier μ_2 as shown in (4.9) is within interval $(0, 1)$. Thus, when $\tau = 0$, $ET < \min\{\bar{x},\hat{x}\}$, and strategy (S1) is applied, the T-periodic solution $(\xi(t),0)$ of (2.2)-(2.4) is orbitally asymptotically stable, which has been shown in Theorem 3.2.

Remark 4.2. If $\tau = 0$, $\hat{x} < ET < \bar{x}$, and (S1) is applied, then the value of μ_2 may be equal to 1, which means that the stability of the periodic solution $(\xi(t),0)$ will change, that is, the bifurcation phenomenon may exist.

According to Remark 4.2, in the following subsection we will discuss the existence of the bifurcation phenomenon of model (2.2)-(2.4) near the PFPS under the assumptions that $\tau = 0$, $\hat{x} < ET < \bar{x}$, and strategy (S1) is applied.

4.2. Bifurcations with respect to p_1

Let p_1 be the bifurcation parameter, where p_1 represents the killing rate of prey by using drug 1 or pesticide 1. Note that in this subsection, we do not require p_1 to be greater than p_2 (the killing rate of prey by using drug 2 or pesticide 2), and p_1 can be taken arbitrarily in interval $(0, 1)$.

We define that both multiplier μ_2 and $EP_1 = (1 - p_1)ET$ are functions of p_1, where the formula of $\mu_2(p_1)$ is shown in (4.9). By analyzing the monotonicity of function $\mu_2(p_1)$ with respect to p_1 and the existence of the root of equation $\mu_2(p_1) - 1 = 0$, the sufficient condition for the existence of bifurcation is given. Then we use the properties of one-parameter family of discrete maps to judge the type of bifurcations.

Taking the derivative of μ_2 with respect to p_1 yields

$$\mu_2'(p_1) = -\mu_2 EP_1' \left(\frac{F_2(EP_1, 0)}{EP_1 \cdot F_1(EP_1, 0)} \right) = \frac{\mu_2}{(1 - p_1)} \frac{F_2(EP_1, 0)}{F_1(EP_1, 0)}. \tag{4.10}$$

Obviously, $\mu_2'(p_1) = 0$ if and only if $F_2((1 - p_1)ET, 0) = F_2(\hat{x}, 0) = 0$, i.e., $p_1 = 1 - \hat{x}/ET$. Moreover,

$$\begin{cases} \text{if } p_1 > 1 - \hat{x}/ET \Rightarrow EP_1 < \hat{x} \Rightarrow F_2(EP_1, 0) < 0 \Rightarrow \mu_2'(p_1) < 0; \\ \text{if } p_1 < 1 - \hat{x}/ET \Rightarrow EP_1 > \hat{x} \Rightarrow F_2(EP_1, 0) > 0 \Rightarrow \mu_2'(p_1) > 0. \end{cases} \tag{4.11}$$

Therefore, function μ_2 monotonically increases with respect to p_1 on interval $(0, 1 - \hat{x}/ET)$ and monotonically decreases on $(1 - \hat{x}/ET, 1)$.

According to (4.9), we have $\lim_{p_1 \to 1^-} \mu_2(p_1) = 0$, and

$$\lim_{p_1 \to 0^+} \mu_2(p_1) = (1 - q_1)(1 - q_2) \exp \left(\int_{EP_2}^{ET} \left(\frac{F_2(x, 0)}{x F_1(x, 0)} \right) dx \right), \tag{4.12}$$

$$\lim_{p_1 \to 1 - \frac{\hat{x}}{ET}} \mu_2(p_1) = (1 - q_1)(1 - q_2) \exp \left(\int_{EP_2}^{ET} \left(\frac{F_2(x, 0)}{x F_1(x, 0)} \right) dx \right) \exp \left(\int_{\hat{x}}^{ET} \left(\frac{F_2(x, 0)}{x F_1(x, 0)} \right) dx \right). \tag{4.13}$$

Combining above equations with the monotonicity of function $\mu_2(p_1)$, we get the following two cases and express them as Remark 4.3.

Remark 4.3. If (4.12) is greater than or equal to 1, then there exists a unique root of $\mu_2(p_1) = 1$, denoted p_{1r}^*, where $\mu_2'(p_{1r}^*) < 0$. That is, the PFPS is locally orbitally asymptotically stable for $p_1 \in (p_{1r}^*, 1)$ while the PFPS is unstable for $p_1 \in (0, p_{1r}^*)$.

If (4.12) is less than 1 and (4.13) is greater than 1, then there exists two roots of $\mu_2(p_1) = 1$, denoted p_{1l}^* and p_{1r}^*, where $p_{1l}^* < 1 - \hat{x}/ET < p_{1r}^*$, $\mu_2'(p_{1l}^*) > 0$, and $\mu_2'(p_{1r}^*) < 0$. That is,

the PFPS is locally orbitally asymptotically stable for $p_1 \in (0, p_{1l}^*) \cup (p_{1r}^*, 1)$ while the PFPS is unstable for $p_1 \in (p_{1l}^*, p_{1r}^*)$.

When $\tau = 0$ and $\hat{x} < ET < \bar{x}$ in this section, the continuity of the Poincaré map $\Phi(u)$, defined by (3.3), is complex. While on $[0, \epsilon^+)$ with ϵ^+ small enough, Φ is still continuously differentiable and as smooth as functions F_1 and F_2. Hence, assume F_1 and F_2 satisfy assumption (H2)', and assume p_1 is the parameter of function G_1, function h and map Φ, then Φ: $[0, \epsilon^+) * (0, 1) \rightarrow [0, +\infty)$ defines a one-parameter family of maps:

$$\Phi(u, p_1) = (1 - q_1)G_2((1 - q_2)G_1(u, p_1)) = (1 - q_1)G_2(h(u, p_1)), \qquad (4.14)$$

which is C^2. Note that functions G_1, G_2 and h are defined in (3.1), (3.2) and (3.6), respectively.

By analyzing the properties of the discrete one-parameter maps $\Phi(u, p_1)$, we obtain the following sufficient conditions for the bifurcation of map $\Phi(u, p_1)$ or system (2.2)-(2.4), as shown in Theorem 4.3.

Theorem 4.3. *Suppose that $\tau = 0$, $\hat{x} < ET < \bar{x}$, (S1) is applied, and (H2)' hold for (2.2)-(2.4). When one of the following two conditions is true, map $\Phi(u, p_1)$ undergoes the transcritical bifurcation at p_1^*:*

(i) *(4.12) is greater than or equal to 1, and (4.18) is not equal to zero for $p_1^* = p_{1r}^*$.*
(ii) *(4.12) is less than 1, (4.13) is greater than 1, and (4.18) is not equal to zero for $p_1^* = p_{1r}^*$ or $p_1^* = p_{1l}^*$.*

Moreover, if $\Phi_{uu}(0, p_1^*) < 0$ (resp., > 0), there appears a stable (resp., an unstable) positive fixed point which is bifurcated from the trivial fixed point 0 (i.e., for system (2.2)-(2.4) using (S1), there appears a stable (resp., an unstable) positive periodic solution which is bifurcated from the PFPS) once p_1 increases and exceeds p_{1l}^* or p_1 is reduced and below p_{1r}^* (resp., p_1 is reduced and below p_{1l}^* or p_1 increases and exceeds p_{1r}^*).

Proof. Assumption (H2)' ensures that map $\Phi(u, p_1)$ is second-order continuously differentiable on $[0, \epsilon^+) * (0, 1)$. Now, to prove this theorem, we only need to verify that $\Phi(u, p_1)$ satisfies the four conditions shown in Lemma 2.4.

It follows from $\dot{y}(t) = yF_2(x, y)$ that $y(t) \equiv 0$ when the initial condition is $y_0 = 0$, which means $G_1(0, p_1) = 0$ and $G_2(0) = 0$. Hence, we have $\Phi(0, p_1) = 0$ holds for all $p_1 \in (0, 1)$.

According to (3.11), the value of $\Phi_u(u, p_1)$ at $u = 0$ is

$$\Phi_u(0, p_1) = (1 - q_1)(1 - q_2) \exp\left(\int_{EP_2}^{ET} G_y(x, 0)dx + \int_{EP_1}^{ET} G_y(x, 0)dx\right) = \mu_2(p_1), \qquad (4.15)$$

where $G_y(x, 0) = F_2(x, 0)/[xF_1(x, 0)]$ and the formula of μ_2 is shown in (4.9). Remark 4.3 tells us that when $\tau = 0$, $\hat{x} < ET < \bar{x}$, assumption (i) or (ii) of Theorem 4.3 hold, then there exists bifurcation point p_{1r}^* or p_{1l}^*, which satisfies $\Phi_u(0, p_{1r}^*) = \mu_2(p_{1r}^*) = 1$ or $\Phi_u(0, p_{1l}^*) = \mu_2(p_{1l}^*) = 1$.

It follows from the formula of $\Phi_u(u, p_1)$ as shown in (3.11) that there are

$$\Phi_{up_1}(u, p_1) = \left(\int_{EP_1}^{ET} G_{yy}(x, y(z, y(x; EP_1, u))) \cdot y_{p_1}(x; EP_1, u)dx - EP_1'G_y(EP_1, u) + \int_{EP_2}^{ET} G_{yy}(x, y(x; EP_2, h(u, p_1)))y_{p_1}(x; EP_2, h(u, p_1))dx \right) \Phi_u(u, p_1),$$

(4.16)

$$y_{p_1}(x; EP_1, 0) = -G(EP_1, 0) \exp\left(\int_{EP_1}^{x} G_y(x, 0)dx \right) EP_1' = 0, \quad y_{p_1}(x; EP_2, h(0, p_1)) = 0.$$

Thus,

$$\Phi_{up_1}(0, p_1) = -\Phi_u(0, p_1)EP_1'G_y(EP_1, 0) = \frac{\mu_2(p_1)}{(1 - p_1)} \frac{F_2(EP_1, 0)}{F_1(EP_1, 0)} = \mu_2'(p_1), \quad (4.17)$$

and for p_{1l}^* and p_{1r}^* as defined in Remark 4.3, $\Phi_{up_1}(0, p_{1l}^*) = \mu_2'(p_{1l}^*) > 0$ and $\Phi_{up_1}(0, p_{1r}^*) = \mu_2'(p_{1r}^*) < 0$.

It follows from (3.12) and (3.9) that the value of $\Phi_{uu}(u, p_1)$ at $u = 0$ and $p_1 = p_1^*$ is

$$\Phi_{uu}(0, p_1^*) = (1 - q_2) \exp\left(\int_{(1-p_1^*)ET}^{ET} G_y(x, 0)dx \right) \int_{EP_2}^{ET} G_{yy}(x, 0) \exp\left(\int_{EP_2}^{x} G_y(x, 0)dx \right) dx$$

$$+ \int_{(1-p_1^*)ET}^{ET} G_{yy}(x, 0) \exp\left(\int_{(1-p_1^*)ET}^{x} G_y(x, 0)dx \right) dx,$$

(4.18)

where p_1^* denotes the root of $\mu_2(p_1) = 1$ and

$$G_y(x, 0) = \frac{F_2}{xF_1}(x, 0), \quad G_{yy}(x, 0) = \frac{2F_{2y}}{xF_1}(x, 0) - \frac{2F_2F_{1y}}{xF_1^2}(x, 0). \quad (4.19)$$

If $\Phi_{uu}(0, p_1^*) \neq 0$, then the map Φ has a transcritical bifurcation at $p_1 = p_{1l}^*$ or $p_1 = p_{1r}^*$ with respect to parameter p_1, further,

- when $\Phi_{uu}(0, p_1^*) < 0$ (see, e.g., Fig. 5.6-(c)-(d)), a stable positive fixed point of map $\Phi(u, p_1)$ (a stable positive periodic solution of (2.2)-(2.4)) appears if $p_1 \in (p_{1l}^*, p_{1l}^* + \epsilon)$ or $p_1 \in (p_{1r}^* - \epsilon, p_{1r}^*)$ with $\epsilon > 0$ small enough, as shown in Fig. 5.7-(d)-(h).

- when $\Phi_{uu}(0, p_1^*) > 0$ (see, e.g., Fig. 5.8-(b)), an unstable positive fixed point of map $\Phi(u, p_1)$ (an unstable positive periodic solution of (2.2)-(2.4)) appears if $p_1 \in (p_{1l}^* - \epsilon, p_{1l}^*)$ or $p_1 \in (p_{1r}^*, p_{1r}^* + \epsilon)$ with $\epsilon > 0$ small enough, as shown graphically in Fig. 5.8-(e). $\square$

5. Applications and numerical simulations

In this section, two examples and their simulations are provided to illustrate the main theorems of the generalized impulsive model (2.2)-(2.4).

5.1. State-dependent feedback control of pest-natural enemy system

Assume that, for model (2.2), $x(t)$ and $y(t)$ are the numbers of pests (prey) and natural enemies (predator) at time t, respectively, and

$$F_1(x, y) = r\left(1 - \frac{x}{K}\right) - \frac{\beta y}{1 + \omega_1 x + \omega_2 \bar{A}}, \quad F_2(x, y) = F_2(x) = \frac{\eta \beta(x + \bar{A})}{1 + \omega_1 x + \omega_2 \bar{A}} - \delta. \quad (5.1)$$

For convenience, we denote the model (2.2)-(2.4) with (5.1) by (5.1)' which is a pest-natural enemy system with state-dependent feedback control and has two pulse strategies: (S1) and (S2).

Here, r is the intrinsic growth rate of pests. K denotes the environmental carrying capacity. $\bar{A}$ denotes the biomass of additional food for natural enemies, and it is assumed to be evenly distributed in the habitat. β is the rate of predator attack on prey. η represents the nutritional value of the prey. δ represents the death rate of the natural enemies. $1/\omega_1$ is the half saturation value for the predation rate. And ω_2 is the quality of additional food. Moreover, the instantaneous killing rate of pesticide i ($i = 1, 2$) for pests and natural enemies are p_i and q_i, respectively. τ represents the instantaneous release amount of natural enemies, which shall not be less than zero. ET represents the economic threshold satisfying $ET < K$ [15]. Especially, when $\bar{A} = 0$, $q_1 = q_2 = 0$, and $p_1 = p_2$, the global dynamic behaviour of (5.1)' is studied in reference [35].

For F_1 and F_2 as shown in (5.1), they satisfy assumptions (H1)-(H3),(H5),(H6),(H8), and (H2)' naturally, where $\bar{x} = K$ and $\bar{y} = r(1 + \omega_2 \bar{A})/\beta$. In addition, a simple calculation shows that if

$$Z_1 := \eta \beta(1 - \omega_1 \bar{A} + \omega_2 \bar{A}) > 0, \ Z_2 := \delta - (\eta \beta - \delta \omega_2)\bar{A} > 0, \ Z_3 := \eta \beta - \delta \omega_1 \neq 0, \quad (5.2)$$

then (H4) and (H7) hold, where $F_{2x} = Z_1/(1 + \omega_1 x + \omega_2 \bar{A})^2 > 0$, and $\hat{x} = Z_2/Z_3 > 0$ when $Z_3 > 0$ while $\hat{x} = +\infty$ when $Z_3 < 0$.

Assume the parameters satisfy the conditions in (5.2) in this section. Then Lemma 2.1 and Lemma 2.2 are also applicable to the corresponding ODE of model (5.1)'. Furthermore, those conclusions about the general impulsive Kolmogorov model (2.2)-(2.4) (such as the properties of Poincaré map, the sufficient conditions for the existence and stability conditions of positive periodic solutions, and the sufficient conditions for the bifurcation of the PFPS) are also applicable to model (5.1)'. Next, we do some numerical simulations with Matlab software, which are somewhat corresponding to Theorems 3.1 to 3.9 (see Fig. 5.1 to Fig. 5.5) and Theorems 4.1 to 4.3 (see Fig. 5.6 to Fig. 5.8).

In Fig. 5.1 to Fig. 5.5, we choose global parameters as follows:

$$r = 1.5, \beta = 0.3, \eta = 0.75, \delta = 0.8, \omega_1 = 0.3, \omega_2 = 0.35, \bar{A} = 0, K = 100, \quad (5.3)$$
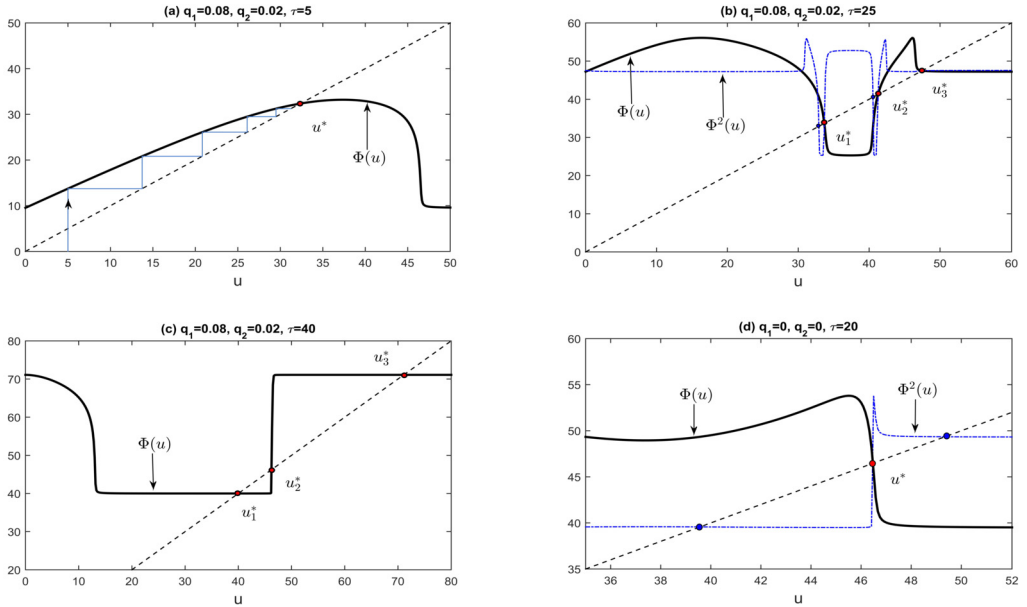
Fig. 5.1. The Poincaré maps Φ of model (5.1)' for the cases (a): $y_{d+1}^+ < y_b^+$; (b): $\tau < y_b^+ < y_{d+1}^+$; (c): $y_b^+ < \tau$; while (d) illustrates the coexistence of order-1 and order-2 periodic solutions. Parameters are shown in (5.3) and (5.4).
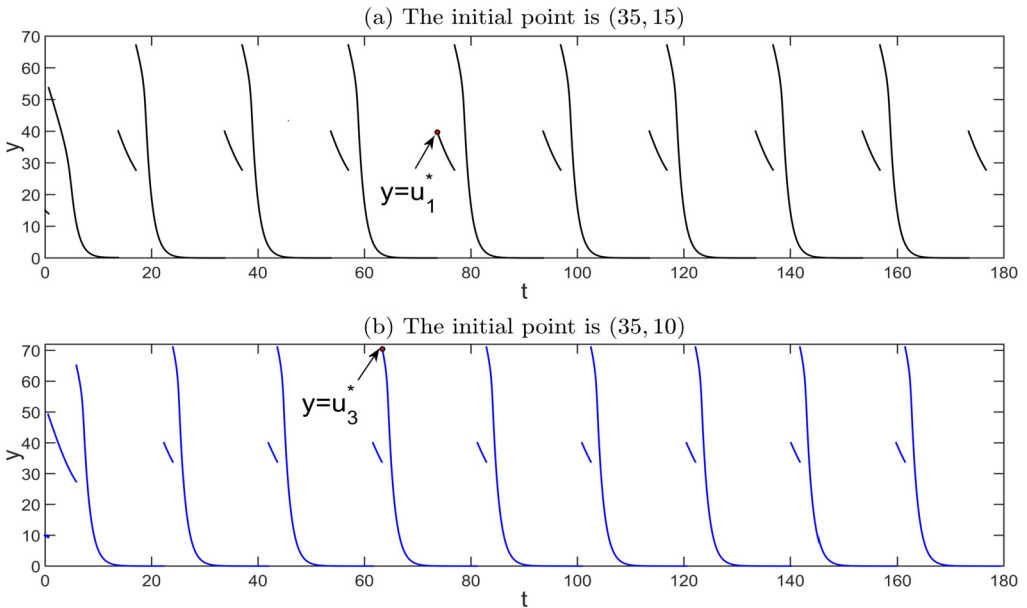

Fig. 5.2. Numerical simulations of $y(t)$ component of the solution $(x(t), y(t))$ to the impulsive system (5.1)'. (a): with the initial condition (35, 15), the solution tends to the periodic solution corresponding to u_1^*; (b): with the initial condition (35, 10), the solution approaches the periodic solution corresponding to u_3^*. Some parameters are $q_1 = 0.08, q_2 = 0.02, \tau = 40$, and others are shown in (5.3) and (5.4).
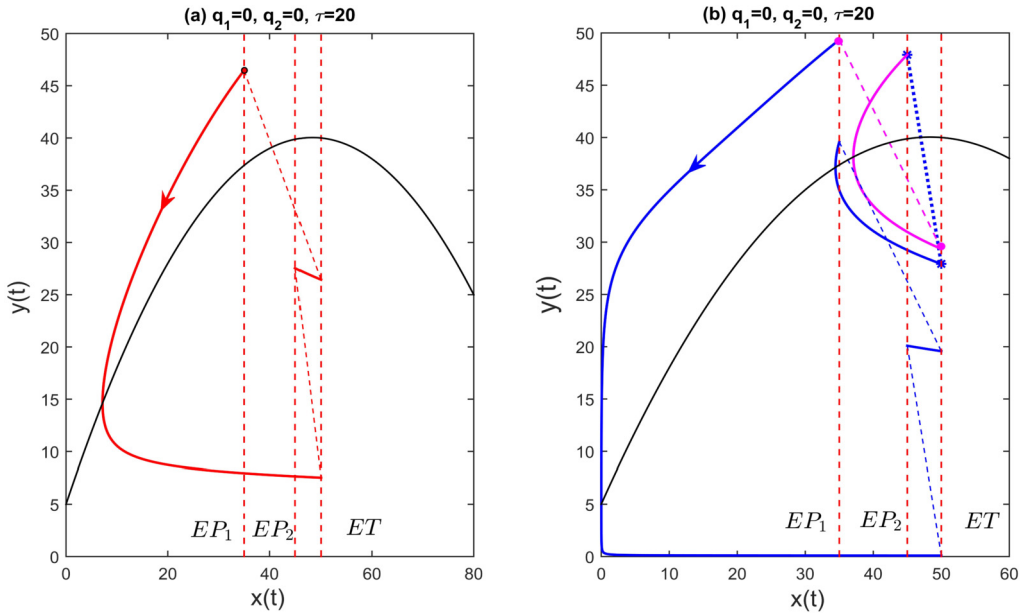
Fig. 5.3. (a): An order-1 periodic solution. (b): An order-2 periodic solution. Parameters are shown in (5.3) and (5.4).

$$ET = 50, \; p_1 = 0.3, \; p_2 = 0.1. \tag{5.4}$$

Simple calculations show that condition (5.2) holds, $\bar{x} = 100$, and $\hat{x} = +\infty$. Thus, the corresponding ODE of model (5.1)' has no positive equilibrium, equilibrium $(\bar{x}, 0)$ is stable, and $ET < \min\{\bar{x}, \hat{x}\}$. Thus, when there is no pulse control, the orbit of model (5.1)' will approach the boundary equilibrium $(100, 0)$ and ecologically, pests will outbreak and the number of pests will settle at the environmental capacity. However, when the impulsive control is implemented repeatedly by (S1), the pest population will always remain below the economic threshold ET, and the existence and stability of periodic solutions of the impulsive system (5.1)' are shown in Theorems 3.1 to 3.9.

When selecting other pulse parameters as $q_1 = 0.08$ and $q_2 = 0.02$, we obtain the diagram of the Poincaré map Φ shown in Fig. 5.1(a)-(c), which indicates that the monotonicity, concavity, and asymptote of Φ are consistent with those described in Theorem 3.1. And Fig. 5.1(a)-(c) shows that the map Φ changes from a single peak to a double peak and finally to an inverted U-shape as τ increases. The solution of (5.1)' as shown in Fig. 5.4 can illustrate that map $\Phi(u)$ (see Fig. 5.1-(b)) is a *bimodal* mapping when $\tau < y_b^+ < y_{d+1}^+$. Fig. 5.1(a)-(d) also shows that when $\tau > 0$ there exists at least one positive fixed point as described in Theorem 3.3, which corresponds to a positive periodic solution of the impulsive model (5.1)'. Moreover, for $\tau = 5$ in Fig. 5.1-(a), the unique fixed point u^* with $u^* < y_d^+$ is globally stable as described in Theorem 3.4. For $\tau = 25$ in Fig. 5.1-(b), the parameters satisfy the condition of Corollary 3.2, and here $\Phi(u)$ has three fixed points, $u_1^* < u_2^* < u_3^*$. Note that in Fig. 5.1-(b), u_1^* and u_2^* are unstable and u_3^* is locally stable, since $|\Phi_u(u_1^*)| > 1$, $|\Phi_u(u_2^*)| > 1$, and $|\Phi_u(u_3^*)| < 1$. However, for $\tau = 40$ in Fig. 5.1-(c), u_1^* and u_3^* are locally stable (bistable), and u_2^* is still unstable, since $|\Phi_u(u_1^*)| < 1$, $|\Phi_u(u_2^*)| > 1$, and $|\Phi_u(u_3^*)| < 1$. The above conclusions can also be observed/confirmed by the method of cobwebbing. Indeed, cobwebbing can give more information about the basin of attraction of a
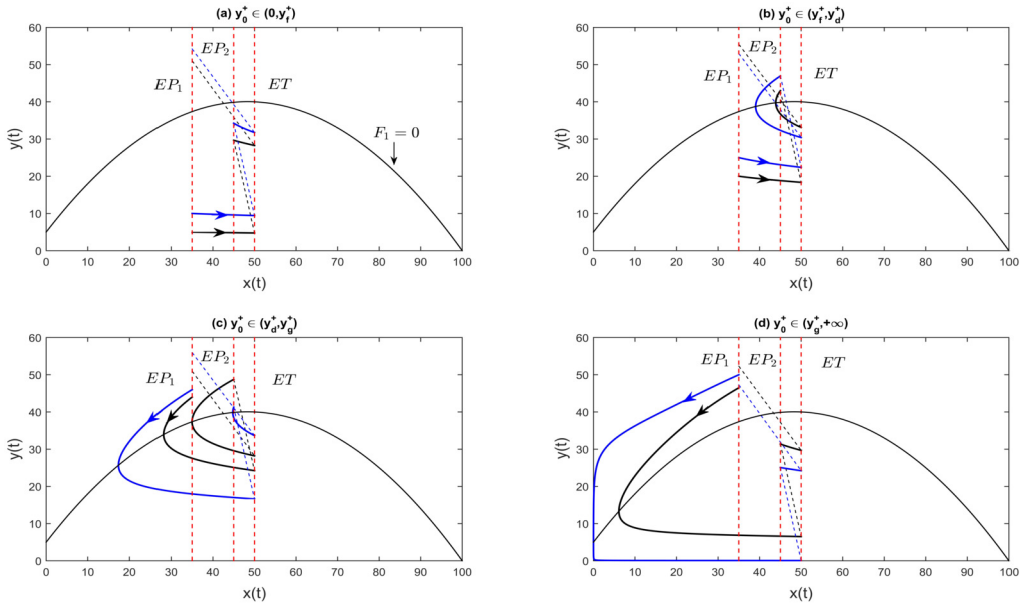
Fig. 5.4. The solutions of (5.1)' to illustrate the monotonicity of $\Phi(u)$ when $\tau < y_b^+ < y_{d+1}^+$. Some parameters are $q_1 = 0.08$, $q_2 = 0.02$, $\tau = 25$, and others are shown in (5.3) and (5.4).

stable equilibrium. For example, applying cobwebbing to Fig. 5.1-(c), we find that the basin of attraction of the fixed point u_3^* is $(0, \bar{u}) \cup (u_2^*, +\infty)$, while the domain of attraction of the fixed point u_1^* is the subinterval of $(\bar{u}, u_2^*)$, where $\Phi(\bar{u}) = u_2^*$.

The numerical results in Fig. 5.1 indicate that with the increase of parameter τ, the number of order-1 periodic solutions and their stabilities become more complicated, and the dynamic behaviours of (2.2)-(2.4) become richer. Fig. 5.1 demonstrate the dynamics of the Poincaré map Φ: existence of order-1 (fixed) and order-2 periodic points of Φ and their stability. Note that each positive stable (unstable) periodic point of Φ corresponds to a stable (unstable) positive periodic solution to the impulsive system (5.1)'. Given a set of initial conditions, the convergence to a periodic solution represented by the corresponding periodic point of Φ (as shown in Fig. 5.1) can be demonstrated by numerical simulations through the time series diagram of solutions to (5.1)'. Taking the case in Fig. 5.1-(c) as an example, when we choose the initial populations to be $(35, 15)$ (resp. $(35, 10)$), one observes that the solution trajectory eventually approaches the periodic solution corresponding to u_1^* (resp. u_3^*), as shown in Fig. 5.2. For both (a) and (b) in Fig. 5.2, the periods of the two periodic solutions of (5.1)' seem to be the same, being approximately 20 time units. Since u_1^* and u_3^* are both *order-1* stable periodic points of Φ, within each period, threshold value of $ET = 50$ for $x(t)$ is reached twice ($1 \times 2 = 2$ times) and accordingly, the controls (C1) and (C2) are each implemented once (refer to Fig. 3.1).

If we choose $q_1 = q_2 = 0$ and $\tau = 20$ then Φ is a bimodal mapping, which has a unique fixed point $u^* = 46.4729$ with $\Phi_u(u^*) < -1$ and a two-point cycle $\Phi^2(u) = u = 39.5690 \neq 49.3456 = \Phi(u)$ as shown in Fig. 5.1-(d). The coexisting order-1 and order-2 periodic solutions of model (5.1)' are shown in Fig. 5.3-(a) and Fig. 5.3-(b), respectively, where the order-1 periodic solution is unstable due to $\Phi_u(u^*) < -1$, and the order-2 periodic solution may be locally orbitally asymptotically stable.
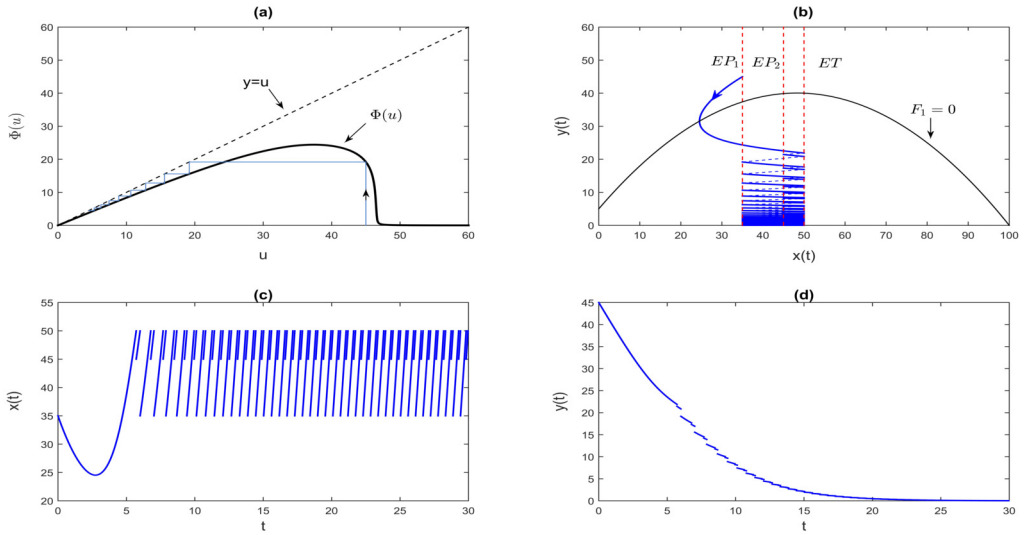
Fig. 5.5. (a) The shape of map Φ. (b) The phase portrait of model (5.1)'. (c) and (d): The time series of pest and natural enemy, respectively. The initial point is $(35, 45)$. Parameters of (5.1)' are $q_1 = 0.08, q_2 = 0.02, \tau = 0$, and others are shown in (5.3) and (5.4).

Fig. 5.5 gives the numerical simulation results with the same the parameter values as those for Fig. 5.1-(b), except that $\tau = 0$. Because $\hat{x} = +\infty$ and $\dot{y}(t) < 0$ for all $x > 0$, there is $y_{d+1}^+ \leq y_{d+1} < y_b^+$ and thus $\Phi(u)$ becomes a unimodal mapping with a unique trivial fixed point, which is globally stable since $|\Phi_u(u = 0 = u^*)| < 1$ and $\lim_{n \to +\infty} \Phi^n(u) = 0$ for all $u \geq 0$ as shown in Fig. 5.5-(a). Hence, it can be seen from Fig. 5.1-(b) and Fig. 5.5-(a) that when τ changes from 25 to zero with $ET < \min\{\bar{x}, \hat{x}\}$, the three positive periodic solutions of the impulsive system (5.1)' disappear and a globally stable PFPS appears, which is consistent with the conclusion described in Theorem 3.2. The solution of model (5.1)' with initial point $(EP_1, 45)$ is shown in Fig. 5.5-(b). Fig. 5.5-(c) indicates that the number of pests will eventually change periodically. Fig. 5.5-(d) not only shows that when $\tau = 0$ and $ET < \min\{\bar{x}, \hat{x}\}$, the number of natural enemies gradually decreases and tends to zero, but also shows that the frequency of using pesticides gradually increases, and finally the pesticides is applied at a periodic time, that is, the state-dependent control will be transformed into periodic control.

Now we take the parameters in Figs. 5.6–5.8 as follows:

$$r = 1.5, \beta = 0.45, \eta = 0.65, \delta = 0.78, \omega_1 = 0.35, \omega_2 = 0.35, \bar{A} = 0, q_1 = q_2 = \tau = 0, \quad (5.5)$$

where $\hat{x} = x^* = 40$. In Fig. 5.6 and Fig. 5.7, $K = 100$ and $ET = 80$ are fixed such that the corresponding ODE of the model (5.1)' has a unique positive equilibrium (x^*, y^*) which is an unstable focus, and $\hat{x} < ET < \bar{x} = 100$. Fig. 5.6-(a) and Fig. 5.6-(b) are the curves of Floquet multiplier $\mu_2(p_1)$, which illustrate that the stability of the PFPS changes near $p_1 = p_{1l}^*$ and $p_1 = p_{1r}^*$. Fig. 5.6-(c) and Fig. 5.6-(d) are the curves of $\Phi_{uu}(0, p_1)$, which show that $\Phi_{uu}(0, p_{1l}^*) < 0$ and $\Phi_{uu}(0, p_{1r}^*) < 0$. The above two inequalities illustrate that under this set of parameters, when the parameter p_1 is reduced and below p_{1r}^* or p_1 increases and exceeds the p_{1l}^*, the PFPS changes from stable to unstable, and a stable positive periodic solution $(\xi(t), \eta(t))$ appears (see Fig. 5.7).
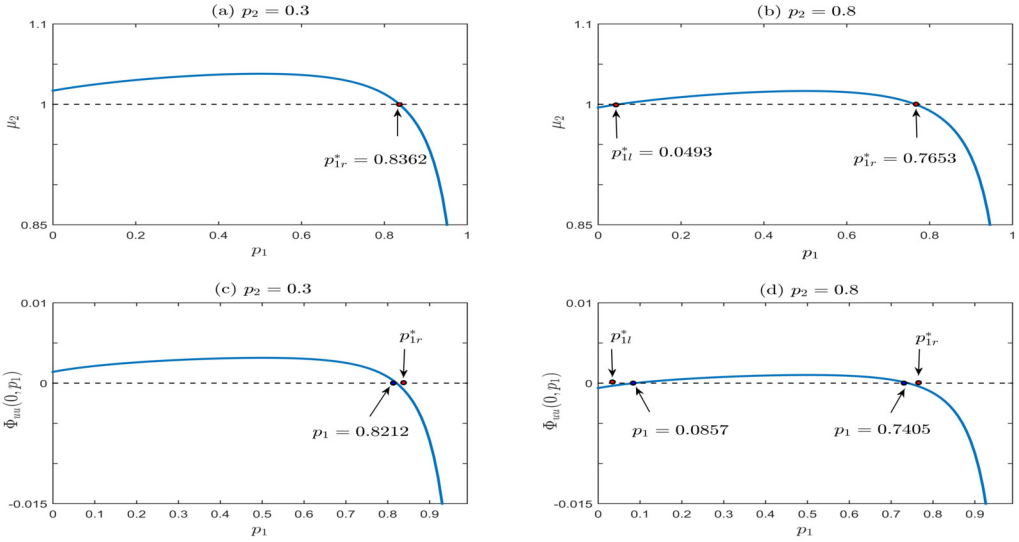
Fig. 5.6. (a) and (b): The curve of Floquet multiplier μ_2 with respect to p_1. (c) and (d): The curve of $\Phi_{uu}(0, p_1)$ with respect to p_1. Parameters of (5.1)' are $K = 100$, $ET = 80$, and others are shown in (5.5).
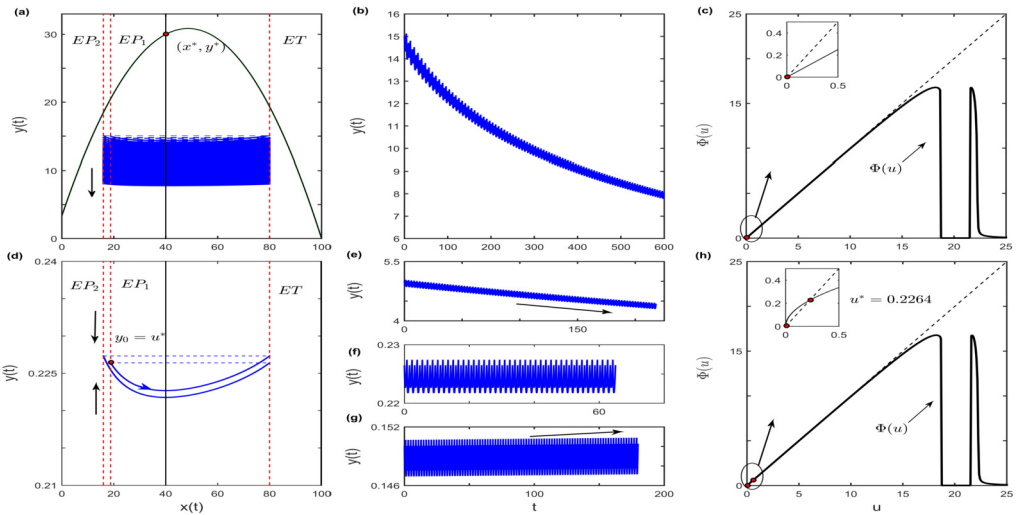

Fig. 5.7. (a) and (d): The phase portrait of system (5.1)'. (b), (e)-(g): The time series of natural enemy. (c) and (h): The curve of Poincaré map Φ. Fixed $p_1 = 0.7654 > p_{1r}^*$ in (a)-(c) and $p_{1l}^* < p_1 = 0.7652 < p_{1r}^*$ in (d)-(h). Parameters of (5.1)' are $K = 100$, $ET = 80$, $p_2 = 0.8$, and others are shown in (5.5).

In Fig. 5.7-(a)-(c), we choose $p_2 = 0.8$ and $p_1 = 0.7654 > p_{1r}^* = 0.7653$ to illustrate the scenario that the PFPS is globally stable. In Fig. 5.7-(d)-(h), we choose $p_2 = 0.8$ and $0.0493 = p_{1l}^* < p_1 = 0.7652 < p_{1r}^*$ such that the PFPS is unstable and there appears a unique positive periodic solution $(\xi(t), \eta(t))$, which is globally stable. The global stability of $(\xi(t), \eta(t))$ is proved by map Φ in Fig. 5.7-(h). Ecologically, $(\xi(t), \eta(t))$ globally stable means that when the initial number of pests and natural enemies meets $x_0 = EP_1$ and $y_0 > 0$, it needs to carry out infinite times
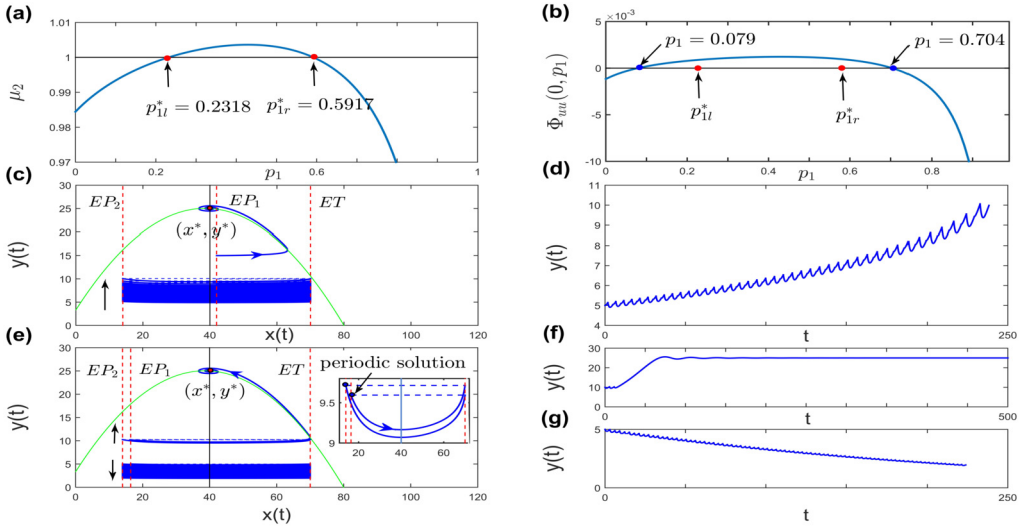
Fig. 5.8. (a) The curve of Floquet multiplier μ_2 with respect to p_1. (b) The curve of $\Phi_{uu}(0, p_1)$ with respect to p_1. (c) and (e): The phase portrait of system (5.1)'. Fixed $p_{1l}^* < p_1 = 0.4 < p_{1r}^*$ in (c) and $p_1 = 0.7652 > p_{1r}^*$ in (e). (d) is a time series of natural enemy corresponding to a trajectory with initial value of $(x_0^+ = EP_1, y_0^+ = 5)$ in (c). (f) and (g) are the time series of natural enemy corresponding to trajectories with initial value of $(x_0^+ = EP_1, y_0^+ = 10)$ and $(x_0^+ = EP_1, y_0^+ = 5)$ in (e), respectively. Parameters of (5.1)' are $K = 80$, $ET = 70$, $p_2 = 0.8$, and others are shown in (5.5).

of comprehensive pest control, and finally the number of the two population changes periodically and tends to $(\xi(t), \eta(t))$.

However, when we change K and ET to $K = 80$ and $ET = 70$, as is shown in Fig. 5.8, the unique positive equilibrium (x^*, y^*) becomes a stable focus and $\hat{x} < ET < \bar{x} = 80$ still holds. Fig. 5.8-(a)-(b) shows that $\mu_2(p_{1l}^*) = 1$, $\mu_2(p_{1r}^*) = 1$, $\Phi_{uu}(0, p_{1l}^*) > 0$, and $\Phi_{uu}(0, p_{1r}^*) > 0$. The above formulas imply that when the parameter p_1 is reduced and below p_{1l}^* or p_1 increases and exceeds the p_{1r}^*, the PFPS changes from unstable to stable, and a positive and unstable periodic solution $(\xi(t), \eta(t))$ appears, which is proved in Fig. 5.8-(c)-(g). Therefore, with the same set of parameters corresponding to Fig. 5.8-(e), the PFPS and the internal positive equilibrium (x^*, y^*) are bistable. Ecologically, this means that when the initial populations satisfy $x_0 = EP_1$ and $y_0 > 0$, either infinite multiple integrated pest control is required, and the final number of pests and natural enemies tends to the PFPS, where the natural enemies become extinct, or only finite pulse control is required and the final number of population tends to (x^*, y^*).

Fig. 5.6 to Fig. 5.8 verify the bifurcation conclusion, that is, under the assumption of Theorem 4.3, the impulsive system (5.1)' has a transcritical bifurcation with respect to parameter p_1 and produces a positive periodic solution near the PFPS.

We can also explore the impact of the efficacy parameter p_1 and the predator release rate parameter τ on the dynamics of the Poincaré map of (5.1)' (hence on (5.1)'). To this end, we fix the parameters as below:

$$r = 1.2, K = 100, \beta = 0.185, \eta = 0.7, \omega_1 = 0.15, \omega_2 = 0.35, \bar{A} = 0, \delta = 0.8, \tag{5.6}$$

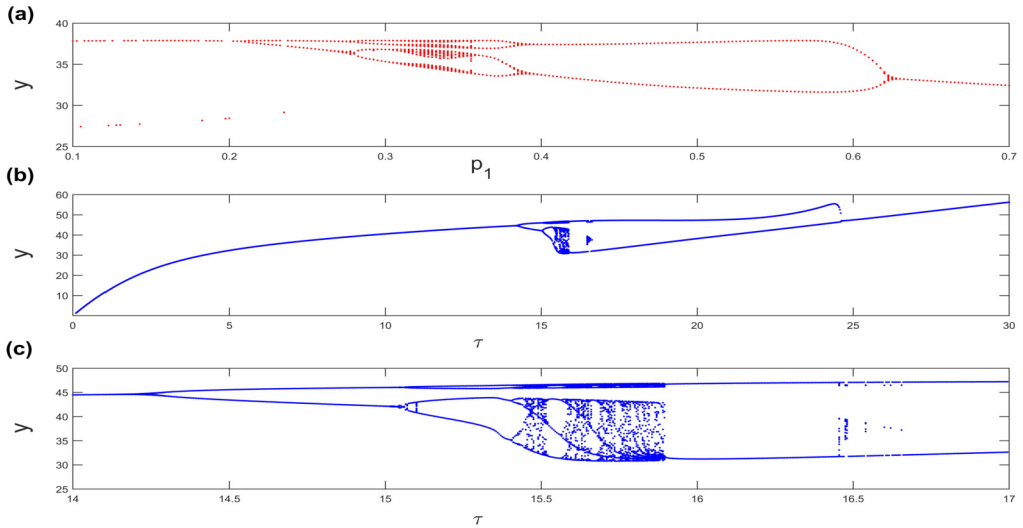$$ET = 68, p_2 = 0.1, q_1 = q_2 = 0, \tau = 15.5, \tag{5.7}$$

Fig. 5.9. (a) Bifurcation diagrams with respect to p_1. Parameters of (a) are shown in (5.6) and (5.7). (b) Bifurcation diagrams with respect to τ with (c) being a zoom-in of (b) near $\tau = 15.5$. Parameters of (b) and (c) are $q_1 = 0.08$, $q_2 = 0.02$, and others are shown in (5.3) and (5.4).

and assume (S1) is applied. With the above fixed, Fig. 5.9-(a) present the bifurcation diagrams for the Poincaré map Φ of (5.1)' with respect to p_1. The diagram shows that when $p_1 = 0.8$, there is a stable order-1 periodic solution of model (5.1)'; when $p_1 = 0.5$ there exists a stable order-2 periodic solution; and an order-4 periodic solution appears when $p_1 = 0.37$. Furthermore, when p_1 decreases to a certain level, then chaos occurs. On the other hand, if we choose $q_1 = 0.08$, $q_2 = 0.02$ and the other parameters as in (5.3) and (5.4), we have the corresponding bifurcation diagram of Φ with respect to τ, given in Fig. 5.9-(b) with $ET < \bar{x} < \hat{x}$. From Fig. 5.9-(b)-(c), we can numerically observe the existence of positive order-1, order-2, order-4, and order-8 periodic orbits for the Poincaré map Φ as τ increases and such a period-doubling bifurcation leads to chaos. It is particularly interesting to observe that when τ is further increased to certain value, there occurs a route from chaos to stable periodic solutions via a cascade of period halving bifurcations.

5.2. State-dependent feedback control of immunogenic tumours

State-dependent pulse therapy is a common method to treat cancer in experiment and clinic [9,4]. For model (2.2)-(2.4), which has two pulse strategies (S1) and (S2), let $x(t)$ and $y(t)$ be the populations of tumour cells and the effector cells, respectively, and

$$F_1(x, y) = r_1 \left(1 - x/K_1\right) - by, \quad F_2(x, y) = cx/(1 + \omega x) - dx - \delta_1 := F_2(x). \qquad (5.8)$$

For convenience, we denote the model (2.2)-(2.4) with (5.8) by (5.8)'. Here, r_1 is the intrinsic growth rate of tumour cells. K_1 represents the carrying capacity. δ_1 is the natural mortality rate of effector cells. b represents the binding rate between tumour cells and effector cells. d denotes the inactivation rate of effector cells. $cx/(1 + \omega x)$ represents the rate at which effector cells are produced due to the presence of tumours. When the diameter of the tumour or the number of

tumour cells is lower than a certain threshold denoted as ET, treatment will not be carried out, but once it reaches the threshold ET, chemotherapy (or radiotherapy, or surgical resection of some tumours) and immunotherapy will be carried out. Here, τ denotes the constant injection rate of effector cells. $p_i \in (0, 1)$ (resp., $q_i \in [0, 1)$) represents the instantaneous removal rate of tumour cells (resp., effector cells) due to chemotherapy or radiotherapy or the surgery. The difference of p_1 and p_2 can represent the switching of chemotherapy drugs or treatment methods. Reference [32] studied the global dynamic behaviour of (5.8)' when $p_1 = p_2$ and $q_1 = q_2 \le 0$.

In this section, F_1 and F_2 always satisfy the assumptions (H1)-(H3), (H5)-(H8), and (H2)' of the Kolmogorov model, where $\bar{x} = K_1$ and $\bar{y} = r_1/b$. Since $F_2(x) < 0 \Longleftrightarrow -d\omega x^2 + (c - \delta_1\omega - d)x - \delta_1 < 0 \Longleftrightarrow -d\omega(x - x_1)(x - x_2) < 0$, where $x_1 = \frac{c - \delta_1\omega - d - \sqrt{\Delta}}{2d\omega}$, $x_2 = \frac{c - \delta_1\omega - d + \sqrt{\Delta}}{2d\omega}$ and $\Delta = (c - \delta_1\omega - d)^2 - 4d\omega\delta_1$, we obtain the following two cases:

(i) If $\Delta < 0$ then there is $F_2(x) < 0$ for all $x \ge 0$ and $\hat{x} = +\infty$, which indicates that (H4) holds true when $\Delta < 0$. For this case, effector cell-free equilibrium $(\bar{x}, 0) = (K_1, 0)$ is a globally stable focus or node for model (2.1). This means that when there is no pulse control, the orbit of model (5.8)' will approach the boundary equilibrium $(\bar{x}, 0)$. Moreover, Theorems 3.1-3.9 on the general model (2.2)-(2.4) apply to this example.

(ii) If $\Delta > 0$, $c - \delta_1\omega - d > 0$, and $0 < x_1 < K_1 < x_2$, then $F_2(x) < 0$ for all $0 \le x < x_1$, and $F_2(x) > 0$ for all $x_1 < x \le K_1$. Model (2.1) has a unique positive equilibrium (x^*, y^*), which is a stable or an unstable focus or node, where $x^* = x_1 = \hat{x} < \bar{x} = K_1$ and (H4) holds. Therefore, Theorem 4.3 (Transcritical bifurcation) still apply to tumour model (5.8)'.

Theorem 3.1 to Theorem 3.9 discuss the existence and stability of order-k ($k \ge 1$) periodic solutions. Theorem 3.3 tells us that when $\tau > 0$ (i.e., when chemotherapy or surgical treatment is combined with immunotherapy), model (5.8)' has at least one positive order-1 periodic solution. When the periodic solution is globally stable, according to the period of periodic solution, the state-dependent pulse therapy can be transformed into fixed time pulse therapy. At this time, it is not necessary to repeatedly monitor the number of tumour cells.

Theorem 4.3 shows that when $\tau = 0$ (cancel immunotherapy) and the parameters of model (5.8)' meet several conditions, (5.8)' will have Transcritical bifurcation with respect to the control parameter p_1 (the killing ratio of chemotherapeutic drug 1 on tumour cells or the resection proportion of tumour tissue by surgical treatment), resulting in stable or unstable positive periodic solutions. When a stable positive periodic solution, an unstable effect cell-free periodic solution $(\xi(t), 0)$, and an unstable positive equilibrium (x^*, y^*) coexist, such as Fig. 5.7-(d), countless therapeutic interventions are needed to control cancer. When $(\xi(t), 0)$ and (x^*, y^*) are bistable and there is an unstable positive periodic solution, such as Fig. 5.8-(e), the frequency of intervention treatment is related to the initial number of tumour cells and effector cells: some need to intervene countless times to control the number of cancer cells below a certain level; some need limited intervention, and the number of tumour cells and effector cells is close to a stable state, which is lower than a certain level; some do not need any treatment, and the number of them is close to a stable equilibrium. This is very consistent with the clinical results of [9,16,38].

6. Conclusion and discussion

In the real world, many harmful or unwanted species often need interventions from humans to control their populations and thereby, reduce their harms. Such controls are usually scheduled

to be implemented in an *impulsive way at given times*. It is known that repeated uses of the same control means can facilitate the resistance to the control, and *combined uses of multiple control means* may help prevent the occurrence of resistance. Meanwhile, most (if not all) harmful or unwanted species (prey) have their natural enemy (predator); and therefore, a control means for the prey species, especially those chemical means, may also have negative effect on the predator species. In this paper, we have formulated a mathematical model system (2.2)-(2.4) for the control of harmful species, which is a result of incorporating into a general predator-prey model the following assumptions: (i) two control means for the harmful species (prey) are available with different efficacies; (ii) the controls are implemented impulsively but based on a threshold for the harmful species (hence, state dependent); (iii) the control may also cause some deaths of the predator and accordingly a constant augmentation of the predator is simultaneously implemented. A theoretical analysis has been done for (2.2)-(2.4) with the strategy (S1): apply the two control means (C1) and (C2) in alternating order. The results show that model (2.2)-(2.4) can demonstrate very rich dynamic behaviour when the alternating control strategy (S1) is applied:

- When $\tau > 0$ and $ET < \min\{\bar{x}, \hat{x}\}$, the study of periodic solution of impulsive system is transformed into the study of fixed points or periodic points of the Poincaré map Φ (the successor function), which is defined on the phase set $\{(x = EP_1, y \geq 0)\}$. By analyzing the properties of this successor function, it is obtained that there must exist a positive order-1 periodic solution of model (2.2)-(2.4), and the sufficient conditions for its global stability are given. The sufficient conditions for the existence of order-2 or order-k ($k \geq 3$) periodic solutions are also discussed. We as well as obtain that when $\tau = 0$ and $ET < \min\{\bar{x}, \hat{x}\}$, the PFPS is globally stable. The above conclusions refer to Theorems 3.1 to 3.9.
- When $\tau = 0$ and $\hat{x} < ET < \bar{x}$, by using the branching lemma of one-dimensional discrete single parameter mapping $\Phi(u, p_1)$, the sufficient conditions for $\Phi(u, p_1)$ to have transcritical bifurcation with respect to parameter p_1 and produce stable or unstable positive periodic solutions are given (see Theorem 4.3). These conclusions are also applicable to the integrated pest management model (5.1)' and the comprehensive tumour treatment model (5.8)'.

Numerically, Figs. 5.1–5.9 confirms that the above conclusions are fully feasible to model (5.1)' and the alternating insecticide strategies can control the number of harmful species within a certain range. However, the rotational drug model has more complex dynamic behaviours than the model using a single drug control (e.g., it can have multiple order-1 periodic solutions). Fig. 5.1-(b) demonstrates a case where (5.1)' has three order-1 periodic solutions together with an order-2 periodic solution. Such a phenomenon has not been reported and observed when only one pest control means is applied (i.e., $p_1 = p_2$ and $q_1 = q_2$). In Fig. 5.1, the appearance of periodic solution shows that the state-dependent pulse can be transformed into periodic pulse without measuring the number or density of harmful species.

With the framework of our model, we can also explore impact of the killing rates. In Fig. 5.7-(a), the killing rate of insecticides is too high, which will lead to the extinction of natural enemies, improve the frequency of pesticides use, and accelerate the development of resistance. This is not conducive to the sustainable control of pests. Fig. 5.7-(d) tells us that appropriate pest killing rate will stabilize the number of pests and natural enemies within a certain range and with periodic change. It also shows that the drug frequency is lower than in Fig. 5.7-(a) — this is conducive to pest control. Fig. 5.8-(e) shows that model (5.1)' may demonstrate a bistable phenomenon, meaning that for different initial numbers of pests and natural enemies, either the solution ap-
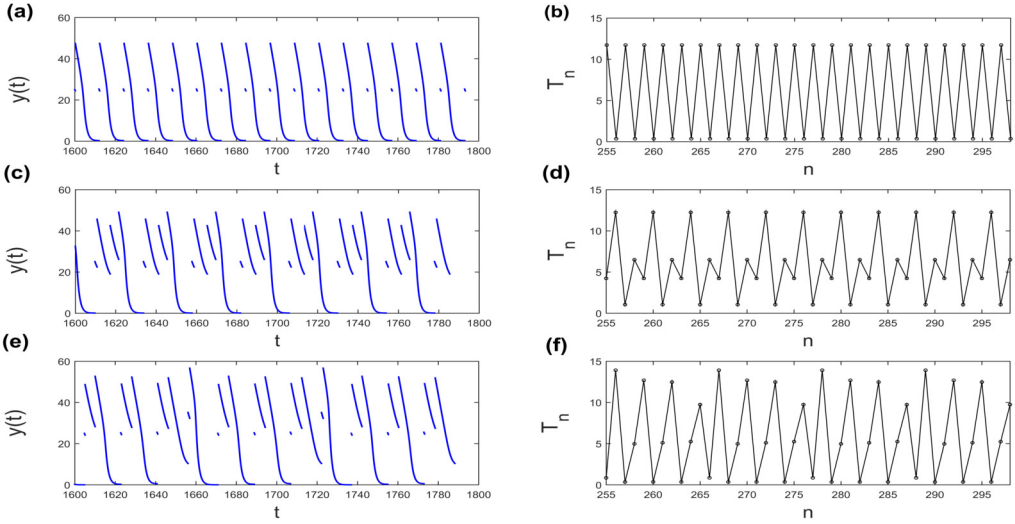
Fig. 6.1. Periodic solution and period of model (5.1)' when two pesticides are used alternately for (a) and (b); only type 1 insecticide is used for (c)-(d); only type 2 insecticide is used for (e)-(f).

proaches the positive equilibrium after a finite number of pest controls, or countless pest controls are required and natural enemies become extinct. Fig. 5.9 illustrates that with the increase of p_1 or τ, the period-doubling bifurcation appears which leads to chaos, and finally the period halving bifurcation occurs.

Fig. 6.1 intends to present some comparison between alternating strategy of two available insecticides, and a strategy of applying only one of the two insecticides. To this end, we consider the scenario of $ET < \bar{x} < \hat{x}$ for which the corresponding baseline ODE for model (5.1)' has no interior equilibrium. We assume that there are two insecticides for consideration in the three control strategies. Let T_n denote the time it takes from the $(n-1)$-th time $x(t)$ hits the threshold ET to the n-th time $x(t)$ hits ET. (a)-(b) presents the numerical results when the first alternating strategy (S1) is applied for model (5.1)'. For the case of only applying one insecticide, (c)-(d) are the results when only applying the first insecticide (i.e., (C1)), while (e)-(f) are results of applying the second insecticide (i.e., (C2)). Parameters are $p_1 = 0.3, p_2 = 0.1, q_1 = 0.08, q_2 = 0.02, ET = 50, \tau = 25$, and others are shown in (5.3); and the initial values are $(x(0), y(0)) = (35, 25)$.

Fig. 6.1-(a) is the plot of $y(t)$ when (S1) is implemented, which also generates Fig. 6.1-(b). From (a)-(b), we see the solution converges to a periodic solution corresponding to two (2) sprayings, with the time lengths between the two consecutive sprayings of the two insecticides being 11.7189 and 0.3533 respectively. Similarly, Fig. 6.1-(c)-(d) shows convergence to a periodic solution corresponding to four (4) sprayings, with the time lengths between four consecutive sprayings being 4.2354, 12.2478, 1.0483, and 6.4943; while Fig. 6.1-(e)-(f) presents a convergence to a stable periodic solution corresponding to eleven (11) sprayings with time lengths between eleven consecutive sprayings being 0.8522, 13.9159, 0.3475, 4.9801, 12.6977, 0.3530, 5.1071, 12.4800, 0.3594, 5.2543, and 9.7426. Note that the least common multiple of 2, 4 and 11 is 44. Calculating the total time lengths after 44 sprayings for the alternating strategy (S1), the strategy of applying only (C1) and the strategy of applying (C2) only, we have
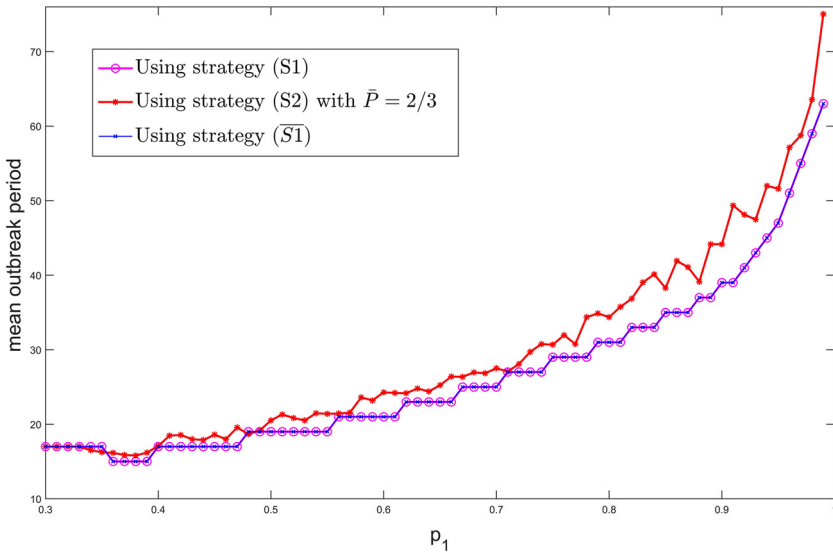
Fig. 6.2. The mean outbreak period of model (5.1)', as a function of p_1. Parameters are $ET = 50, q_1 = 0.04, q_2 = 0.02, p_2 = 0.3, \tau = 5$, and others are shown in (5.3). (For interpretation of the colours in the figure(s), the reader is referred to the web version of this article.)

$$(11.7189 + 0.3533) \times 22 = 265.5884 \qquad \text{(for strategy (S1))}$$

$$> (0.8522 + 13.9159 + 0.3475 + 4.9801 + 12.6977 + 0.3530 + 5.1071 + 12.4800 + 0.3594$$

$$+ 5.2543 + 9.7426) \times 4 = 264.3592 \qquad \text{(for applying (C2) only)}$$

$$> (4.2354 + 12.2478 + 1.0483 + 6.4943) \times 11 = 264.2838 \qquad \text{(for applying (C1) only)}.$$

This comparison of the lengths of keeping the pest under control indicates that the alternating strategy is the best among the three. Such a conclusion is consistent with the theory that the likelihood of a population developing resistance to two or more pesticides, each from a different chemical group with different modes of action, is significantly less than the likelihood that a population could develop resistance to only one of the pesticides [36].

We point out that we have not done a theoretical analysis for the random strategy (S2) because, as we mentioned in the introduction, an analysis would involve some probability argument to reflect the randomness of (S2). However, we have performed some numerical simulations by which we can have a comparison with (S1) and $(\overline{S1})$ in some aspect. To this end, we choose the parameter values in (5.3) with which the corresponding ODE of model (5.1)' has no interior equilibrium. Now, we further choose $ET = 50, q_1 = 0.04, q_2 = 0.02, p_2 = 0.3, \tau = 5$. Note that when using strategy (S2) for model (5.1)', the higher killing rate of insecticide 1 makes it more likely to be used by agricultural workers than insecticide 2. Thus, it is reasonable to assume $\bar{P} > 1/2$. For demonstration, we choose $\bar{P} = 2/3$, that is, when the number of pests reaches ET, insecticide 1 and insecticide 2 are selected with probabilities of 2/3 and 1/3 respectively. The alternating strategies (S1) and $(\overline{S1})$ are essentially the same, except the order in which the two pesticides are selected differs. Defining them as (S1) and $(\overline{S1})$ is only for the convenience of facilitating theoretical analysis and numerical simulation. As such, the effect of these two control strategies should be the same, and this is reflected by the full overlap of the pink and blue curves

in Fig. 6.2. In Fig. 6.2, simulations are run for 300 pest outbreak events to rule out transients, and the last 100 points of sequence T_n are used to determine the mean outbreak period. Fig. 6.2 also clearly shows that strategy (S2) is the best since the *mean outbreak period* of the pest when two pesticides are applied randomly by (S2) is longer than that when the alternating strategy (S1) or $(\overline{S1})$ is used. This is consistent with the theory that the rotation of pesticides should not be too regular—the more regular, the more likely to cause resistance [8,10]. Practitioners should make certain adjustments according to the actual situation when using pesticides to control pests. In strategy (S2), insecticide 1 is used more frequently than insecticide 2. But in such a case, the use frequency of insecticide 1 should not be too high; otherwise, excessive dependence on insecticide 1 will also facilitate occurrence of drug resistance. It is expected that the balance between the frequency of using insecticide 1 and insecticide resistance is complex but will play a crucial role. We leave this and the topics related to (S2) for future research projects.

We point out that this paper intends to establish a theoretical framework for a class of problems that involve state-dependent impulsive controls of population of an unwanted species. The motivation is pest control and tumour inhibiting in the presence of a predator species (e.g., natural enemy or effector cells) and thus, the predator-prey type interaction is considered beyond the control. Accordingly, we use a general predator-prey ODE systems as the baseline system. As such, this work is of theoretical nature and effort was not made to gather related data to valid the model for a particular problem. The values of the parameters in the numerical simulations, together with the simulations, are mainly for the purpose of demonstrating our analytical results.

A key step in this work is to reduce the 2-D Poincaré map of the 2-D ODE model with state-dependent impulsive controls switching between two means into a 1-D function (also called Poincaré), in the form of weighted composition. This is possible mainly because the dynamics of the baseline predator-prey ODE system (2.1) is fully understood and can be conveniently described in terms of the phase-plane portrait. We believe this framework can be easily expanded to the population controls of two competitive or cooperative species by replacing the baseline predator-prey ODE system with a 2-D competitive or cooperative ODE system for which, the dynamics can also be conveniently described by the phase portrait technique (well-known results also exist). However, when the baseline ODE system is a *three or higher dimensional* ODE system, it is, in general, very difficult to determine the direction of its vector field. Thus, generalization of the framework in this paper to a similar problem with the baseline ODE system having a higher (than 2) dimension, will face great challenges in determining and simplifying/reducing the Poincaré map to simpler lower dimensional map. This does not exclude some special higher dimensional systems for which this method can work out.

Data availability

No data was used for the research described in the article.

Acknowledgments

Appendix A. The proof of Theorem 3.5

Proof. Under the assumptions of Theorem 3.5, map $\Phi(u)$, as shown in Fig. 3.2-(a), is increasing and concave down on $[0, y_d^+]$, and decreasing on $(y_d^+, +\infty)$, which is proved in Theorem 3.1(ii). There is no fixed point on $[0, y_d^+]$ due to $\Phi(0) > 0$, $\Phi(y_d^+) > y_d^+$, and Φ is concave down on $[0, y_d^+]$. There exists a unique $u^* \in (y_d^+, +\infty)$ satisfying $\Phi(u^*) = u^*$, since $\Phi(u)$ decreases on $(y_d^+, +\infty)$, $\Phi(y_d^+) > y_d^+$, and there exists a w large enough such that $\Phi(w) < w$.

(i) We claim that the fixed point u^* of unimodal map Φ is globally stable if $\Phi^2(u) > u$ for all $u \in [y_d^+, u^*)$. Let us divide $(0, +\infty)$ into three subintervals: $[y_d^+, u^*)$, $(0, y_d^+)$, and $(u^*, +\infty)$.

- When $u \in [y_d^+, u^*)$, because $\Phi(u^*) = u^*$, $\Phi(u)$ is monotonically decreases on $[y_d^+, +\infty)$, and $\Phi^2(\bar{u}) > \bar{u}$ for all $\bar{u} \in [y_d^+, u^*)$, then we have

$$y_d^+ \le u < \Phi^2(u) < \Phi^4(u) < \cdots < u^* = \Phi(u^*) < \cdots < \Phi^3(u) < \Phi(u).$$

  Using mathematical recursion, one yields that $\Phi^{2n}(u)$ monotonically increases toward u^* as $n \to +\infty$ and $\Phi^{2n+1}(u)$ monotonically decreases toward u^* as $n \to +\infty$.
- When $u \in (0, y_d^+)$, there exists a m_1 such that $u^* \le \Phi^{m_1}(u) \le \Phi(y_d^+)$. Moreover, there is a $\hat{u}_1 \in [y_d^+, u^*]$ satisfying $\Phi^{m_1}(u) = \Phi(\hat{u}_1)$. Similar to the above case, $\lim_{n \to \infty} \Phi^n(u) = u^*$ holds.
- When $u \in (u^*, +\infty)$, $\Phi(u) < u^*$ and there exists a $\hat{u}_2 \in (0, y_d^+)$ such that $\Phi(u) = \Phi(\hat{u}_2)$. Thus, similar to the above second case, $\lim_{n \to \infty} \Phi^n(u) = u^*$.

(ii) When $u \in (0, y_d^+)$ or $u \in (u^*, +\infty)$, there must exists a m_3 such that $\Phi^{m_3}(u) \in [u^*, \Phi(y_d^+)]$. Further, $\Phi^{m_3+1}(u) \in [\Phi^2(y_d^+), u^*] \subseteq [y_d^+, u^*]$ due to Φ monotonically decreases on $[u^*, +\infty)$ and $\Phi^2(y_d^+) \ge y_d^+$. Thus, we need to discuss the convergence of column $\{\Phi^n(u)\}$ when $u \in (y_d^+, u^*)$. For convenience, denote $\Phi^n(u) = u_n$ in the following.

When $u \in (y_d^+, u^*)$, because $\Phi(u)$ is monotonically decreases on $[y_d^+, +\infty)$ and $\Phi^2(y_d^+) \ge y_d^+$, there are $y_d^+ < u < u^* < u_1 < \Phi(y_d^+)$ and $y_d^+ < u_2 < u^*$. Combining the above with the relationship between u and u_2, we have the following three situations: (M1) $u_2 = u < u^* < u_1$, (M2) $u < u_2 < u^* < u_1$, and (M3) $y_d^+ < u_2 < u < u^* < u_1 < \Phi(y_d^+)$.

- When (M1) occurs, map Φ has a two-point cycle.
- When (M2) occurs, there is $u < u_2 < u_4 < \cdots < u^* < \cdots < u_3 < u_1$. Thus, $\{u_{2n}\}$ and $\{u_{2n+1}\}$ are monotonically bounded point sequences and $\lim_{n \to +\infty} u_{2n} \le u^* \le \lim_{n \to +\infty} u_{2n+1}$. If $\lim_{n \to +\infty} u_{2n} \neq \lim_{n \to +\infty} u_{2n+1}$, then map Φ has a two-point cycle.
- When (M3) occurs, there is $y_d^+ < \cdots < u_4 < u_2 < u < u^* < u_1 < u_3 < \cdots < \Phi(y_d^+)$. Thus, $\lim_{n \to \infty} u_{2n} \neq \lim_{n \to \infty} u_{2n+1}$ and Φ has a two-point cycle.

Now, we have proved that, Φ has a globally stable fixed point if and only if case (M2) occurs for all $u \in (y_d^+, u^*)$ and $\lim_{n \to +\infty} u_{2n} \equiv \lim_{n \to +\infty} u_{2n+1}$. Otherwise, a two-point cycle coexists with the fixed point.

(iii) According to $\Phi(u)$ is continuous on $[0, +\infty)$, function $\Phi^3(u) - u$ is also continuous on $[0, +\infty)$. Obviously, $\Phi^3(0) > 0$. Under the assumption of $\Phi^2(y_d^+) < y_{v_1}^+$, where $y_{v_1}^+ = \min\{u| \Phi(u) = y_d^+\}$, there is $\Phi^3(y_{v_1}^+) = \Phi^2(y_d^+) < y_{v_1}^+$. Hence, there is a $u^{***} \in (0, y_{v_1}^+)$ such

that $\Phi^3(u^{***}) = u^{***}$. Moreover, it follows from $u^{***} < y_{v_1}^+ < y_d^+ < u^*$ that $u^{***} \neq u^*$ and map Φ has a periodic point with period 3.

For the continuous self mapping Φ defined on $[0, +\infty)$, because there is a periodic point with period 3, there is also a periodic point with period k, where $k = 1, 2, 3, \ldots$, which is guaranteed by Sharkovskii' theorem [29]. The above indicates that the impulsive model (2.2)-(2.4) has order-k ($k = 1, 2, 3, \ldots$) periodic solutions and has chaotic attractor, which is guaranteed by Li-Yorke' theorem [21]. $\square$

Appendix B. The proof of Theorem 3.9

Proof. Under the assumption of Φ has a unique fixed point u^*, one yields (I): $\Phi(u) > u$ for all $u < u^*$ and $\Phi(u) < u$ for all $u > u^*$. Theorem 3.1(iii) also tells us that (II): $\Phi(u)$ is decreasing on $[y_f^+, u^*)$. In the following, we prove the convergence of $\{\Phi^n(u)\}$ when $u \in [y_f^+, u^*)$, or $u \in [0, y_f^+)$, or $u \in (u^*, +\infty)$.

(i) For all $u \in [y_f^+, u^*)$, $u^* < \Phi(u)$ because of (II). Further, either $\Phi^n(u) \geq u^*$ for all $n \geq 1$, which indicates that $\{\Phi^n(u)\}$ is decreasing toward u^* as $n \to +\infty$ because of (I), or there exists a $m \geq 2$ such that

$$\Phi^m(u) < u^* < \Phi^{m-1}(u) < \cdots < \Phi(u) \leq \Phi(y_f^+). \tag{B.1}$$

It follows from the assumption of $\Phi^2(u) > u$ for all $u \in [y_f^+, u^*)$ that $u < \Phi^m(u)$ is true if $m = 2$. If $m > 2$, then there exists a $y \in [y_f^+, u^*)$ such that $\Phi(y) = \Phi^{m-1}(u)$ and $y < \Phi^2(y) = \Phi^m(u)$. Moreover, the number y is greater than u since (II), $u \in [y_f^+, u^*)$, $y \in [y_f^+, u^*)$, and $\Phi(y) = \Phi^{m-1}(u) < \Phi(u)$, as shown in (B.1). Now, we get

$$y_f^+ \leq u < \Phi^m(u) < u^* < \Phi^{m-1}(u) < \cdots < \Phi(u). \tag{B.2}$$

It can be seen from the above analysis that when $u \in [y_f^+, u^*)$, either there is a m such that $\Phi^{m+j}(u)$ is decreasing toward u^* as $j \to +\infty$, or there is a subsequence $\{m_j\}$ of $\{m\}$ such that $\Phi^{m_j}(u)$ is increasing toward u^* as $j \to +\infty$. It remains to prove the convergence of $\{\Phi^n(u)\}$ for the last case.

First, function $\Phi(u)$ is continuous, which tells us that for any $\epsilon > 0$, there exists a δ with $0 < \delta < \epsilon$ such that $|\Phi(u) - u^*| < \epsilon$ for all $|u - u^*| < \delta$.

Point sequence $\{\Phi^{m_j}(u)\}$ converges to u^* as $j \to +\infty$, that is, for any δ with $0 < \delta < \epsilon$, there exists a N such that $|\Phi^{m_j}(u) - u^*| < \delta$ for all $j > N$, which implies that $|\Phi^{m_j+1}(u) - u^*| < \epsilon$ for all $j > N$ and $u \in [y_f^+, u^*)$. Note that there are $m_j + 1 < m_{j+1}$ and

$$y_f^+ \leq u < \Phi^{m_j}(u) < \Phi^{m_{j+1}}(u) < u^* < \Phi^{m_{j+1}-1}(u) < \cdots < \Phi^{m_j+1}(u) < \Phi(u) \tag{B.3}$$

due to (I) and (B.2).

Hence, for any $\epsilon > 0$, there exists a N such that $|\Phi^n(u) - u^*| < \epsilon$ for all $n > m_N$ and $u \in [y_f^+, u^*)$. That is, the convergence of point sequence $\{\Phi^n(u)\}$ is proved when $u \in [y_f^+, u^*)$.

(ii) For all $u \in [0, y_f^+)$, then either $\Phi^n(u) \leq u^*$ for all $n \geq 1$, which means $\Phi^n(u)$ increases toward u^* as $n \to +\infty$ because of (I), or there exists a k_1 such that $u^* < \Phi^{k_1}(u) \leq \Phi(y_f^+)$,

which implies that there exists a $y \in [y_f^+, u^*)$ such that $\Phi(y) = \Phi^{k_1}(u)$. Therefore, similar to above situation (i), $\Phi^n(u)$ converges to u^* as $n \to +\infty$.

(iii) For all $u \in (u^*, +\infty)$, then either $\Phi^n(u) \geq u^*$ for all $n \geq 1$, which means that $\Phi^n(u)$ decreases toward u^* as $n \to +\infty$ because of (I), or there exists a k_2 such that $\Phi^{k_2}(u) < u^*$, then similar to situations (i) and (ii), there is $\lim_{n\to+\infty} \Phi^n(u) = u^*$. This completes the proof. $\quad\square$

References

[1] F. Albrecht, H. Gatzke, A. Haddad, N. Wax, The dynamics of two interacting populations, J. Math. Anal. Appl. 46 (1974) 658–670.
[2] K.O. Alfarouk, C.M. Stock, S. Taylor, M. Walsh, A.K. Muddathir, D. Verduzco, A.H.H. Bashir, O.Y. Mohammed, G.O. Elhassan, S. Harguindey, Resistance to cancer chemotherapy: failure in drug response from ADME to P-gp, Cancer Cell Int. 15 (2015) 1–13.
[3] B.B.C. News, Chemo 'undermines itself' through rogue response, https://www.bbc.com/news/health-19111700, 2012.
[4] S. Broomfield, A. Currie, R.G. Van der Most, M. Brown, I. Van Bruggen, B.W.S. Robinson, R.A. Lake, Partial, but not complete, tumor-debulking surgery promotes protective antitumor memory when combined with chemotherapy and adjuvant immunotherapy, Cancer Res. 65 (2005) 7580–7584.
[5] Y.J. Bor, Optimal pest management and economic threshold, Agric. Syst. 49 (1995) 113–133.
[6] T. Cheng, S. Tang, R.A. Cheke, Threshold dynamics and bifurcation of a state-dependent feedback nonlinear control susceptible-infected-recovered model, J. Comput. Nonlinear Dyn. 14 (2019) 1–14.
[7] P. Cull, Global stability of population models, Bull. Math. Biol. 43 (1981) 47–58.
[8] R. Cloyd, How to maximize pesticide efficacy, https://www.greenhousemag.com/article/maximize-the-efficacy-of-pesticides/, 2017.
[9] B.G. Duffey, P.L. Choyke, G. Clenn, R.L. Grubb, D. Venzon, W.M. Linehan, M.M. Walther, The relationship between renal tumor size and metastases in patients with von Hippel-Lindau disease, J. Urol. 172 (2004) 63–65.
[10] DoMyOwn, Why rotate your insecticide treatments?, https://www.domyown.com/the-importance-of-insecticide-rotation-a-809.html.
[11] M.E. Fisher, B.S. Goh, T.L. Vincent, Some stability conditions for discrete-time single-species models, Bull. Math. Biol. 41 (1979) 861–875.
[12] D.J. Finney, Probit Analysis, 2nd ed., Cambridge University Press, 1952.
[13] J.M. Grandmont, Nonlinear difference equations, bifurcations and chaos: an introduction, Res. Econ. 62 (2008) 122–177.
[14] M.M. Gubin, X. Zhang, H. Schuster, E. Caron, J.P. Ward, T. Noguchi, Y. Ivanova, J. Hundal, C.D. Arthur, W.J. Kreber, G.E. Mulder, M. Toebes, M.D. Vesely, S.S.K. Lam, A.J. Korman, J.P. Allison, G.J. Freeman, A.H. Sharpe, E.L. Pearce, T.N. Schumacher, R. Aebersold, H.G. Rammensee, C.J.M. Melief, E.R. Mardis, R.W.E. Gillanders, M.N. Artyomov, R.D. Schreiber, Checkpoint blockade cancer immunotherapy targets tumour-specific mutant antigens, Nature 545 (2014) 577–581.
[15] J.C. Headley, Defining the Economic Threshold, National Academy of Sciences, Washington, D.C., 1972.
[16] J.C. Herring, E.G. Enquist, A. Chernoff, W.M. Linehan, P.L. Choyke, M.M. Walther, Parenchymal sparing surgery in patients with hereditary renal cell carcinoma: ten year experience, J. Urol. 165 (2001) 777–781.
[17] M. Huang, J. Li, X. Song, H. Guo, Modeling impulsive injections of insulin: towards artificial Pancreas, SIAM J. Appl. Math. 72 (2012) 1524–1548.
[18] Y. Huang, A note on stability of discrete population models, Math. Biosci. 95 (1989) 189–198.
[19] A.N. Kolmogorov, Sulla teoria di Volterra della lotta per lésistenza, G. Ist. Ital. Attuari 7 (1936) 74–80.
[20] J. Liang, S. Tang, Optimal dosage and economic threshold of multiple pesticide applications for pest control, Math. Comput. Model. 51 (2010) 487–503.
[21] T.Y. Li, J.A. Yorke, Period three implies chaos, Am. Math. Mon. 82 (1975) 985–992.
[22] S.S. Lynch, Tolerance and resistance to drugs, https://www.merckmanuals.com/home/drugs/factors-affecting-response-to-drugs/tolerance-and-resistance-to-drugs, 2022.
[23] L. Nie, Z. Teng, B. Guo, A state dependent pulse control strategy for a SIRS epidemic system, Bull. Math. Biol. 75 (2013) 1697–1715.
[24] B. Norquist, K.A. Wurz, C.C. Pennil, R. Garcia, J. Gross, W. Sakai, B.Y. Karlan, T. Taniguchi, E.M. Swisher, Secondary somatic mutations restoring BRCA1/2 predict chemotherapy resistance in hereditary ovarian carcinomas, J. Clin. Oncol. 29 (2011) 3008–3015.

[25] J.C. Panetta, A logistic model of periodic chemotherapy, Appl. Math. Lett. 8 (1995) 83–86.

[26] A. Rescigno, I.W. Richardson, The struggle for life. I. Two species, Bull. Math. Biophys. 29 (1967) 377–388.

[27] G. Rosenkranz, On global stability of discrete population models, Math. Biosci. 64 (1983) 227–231.

[28] J. Ruberson, H. Nemoto, Y. Hirose, Pesticides and conservation of natural enemies in pest management, Conserv. Biol. Control 20 (1998) 207–220.

[29] A.N. Sharkovskii, Co-existence of cycles of a continuous mapping of the line into itself, Ukr. Math. J. 16 (1964) 61–71.

[30] P.S. Simeonov, D.D. Bainov, Orbital stability of the periodic solutions of autonomous systems with impulse effect, Int. J. Syst. Sci. 19 (1988) 2561–2585.

[31] B. Tang, Q. Li, Y. Xiao, S. Sivaloganathan, A novel hybrid model of tumor control, combining pulse surveillance with tumor size-guided therapies, Appl. Math. Model. 104 (2022) 259–278.

[32] B. Tang, Y. Xiao, S. Tang, R.A. Cheke, A feedback control model of comprehensive therapy for treating immunogenic tumours, Int. J. Bifurc. Chaos 26 (2016) 1–22.

[33] S. Tang, R.A. Cheke, Models for integrated pest control and their biological implications, Math. Biosci. 215 (2008) 115–125.

[34] S. Tang, C. Li, B. Tang, X. Wang, Global dynamics of a nonlinear state-dependent feedback control ecological model with a multiple-hump discrete map, Commun. Nonlinear Sci. Numer. Simul. 79 (2019) 1–20.

[35] S. Tang, B. Tang, A. Wang, Y. Xiao, Holling II predator-prey impulsive semi-dynamic model with complex Poincaré map, Nonlinear Dyn. 81 (2015) 1575–1596.

[36] United States Environmental Protection Agency, Slowing and combating pest resistance to pesticides, https://www.epa.gov/pesticide-registration/slowing-and-combating-pest-resistance-pesticides, 2021.

[37] J. van Lenteren, Success in biological control of arthropods by augmentation of natural enemies, in: Biological Control: Measures of Success, 2000, pp. 77–103.

[38] M.M. Walther, P.L. Choyke, G. Glenn, J.C. Lyne, W. Rayford, D. Venzon, W.M. Linehan, Renal cancer in families with hereditary renal cancer: prospective analysis of a tumor size threshold for renal parenchymal sparing surgery, J. Urol. 161 (1999) 1475–1479.

[39] J. Xu, Y. Tian, H. Guo, X. Song, Dynamical analysis of a pest management Leslie-Gower model with ratio-dependent functional response, Nonlinear Dyn. 93 (2018) 705–720.

[40] J. Yang, S. Tang, R.A. Cheke, Modelling pulsed immunotherapy of tumour-immune interaction, Math. Comput. Simul. 109 (2015) 92–112.

[41] J. Yang, S. Tang, R.A. Cheke, The regulatory system for diabetes mellitus: modeling rates of glucose infusions and insulin injections, Commun. Nonlinear Sci. Numer. Simul. 37 (2016) 305–325.

[42] Q. Zhang, B. Tang, T. Cheng, S. Tang, Bifurcation analysis of a generalized impulsive Kolmogorov model with applications to pest and disease control, SIAM J. Appl. Math. 80 (2020) 1796–1819.

[43] Q. Zhang, B. Tang, S. Tang, Vaccination threshold size and backward bifurcation of SIR model with state-dependent pulse control, J. Theor. Biol. 455 (2018) 75–85.

[44] Q. Zhang, S. Tang, Bifurcation analysis of an ecological model with nonlinear state-dependent feedback control by Poincaré map defined in phase set, Commun. Nonlinear Sci. Numer. Simul. 108 (2022) 1–25.